Asymptotics of Plancherel measures for the infinite-dimensional unitary group

Alexei Borodin Jeffrey Kuan

June 29, 2018

Abstract

We study a two-dimensional family of probability measures on infinite Gelfand-Tsetlin schemes induced by a distinguished family of extreme characters of the infinite-dimensional unitary group. These measures are unitary group analogs of the well-known Plancherel measures for symmetric groups.

We show that any measure from our family defines a determinantal point process on $\mathbb{Z}_+ \times \mathbb{Z}$, and we prove that in appropriate scaling limits, such processes converge to two different extensions of the discrete sine process as well as to the extended Airy and Pearcey processes.

1 Introduction

Let $S(n)$ be the symmetric group of degree n. Denote by $\mathbb{Y}_n$ the set of partitions of n or, equivalently, the set of Young diagrams with n boxes. It is well known that complex irreducible representations of $S(n)$ are parameterized by elements of $\mathbb{Y}_n$; we denote by $\dim\lambda$ the dimension of the irreducible representation corresponding to λ. The probability distribution

$$\mathrm{Prob}\{\lambda\} = \frac{\dim^2\lambda}{n!}, \qquad \lambda\in\mathbb{Y}_n,$$

on $\mathbb{Y}_n$ is called the *Plancherel measure* for $S(n)$. The Plancherel weight of $\lambda\in\mathbb{Y}_n$ is the relative dimension of the isotypic component of the regular representation of $S(n)$, which transforms according to the irreducible representation corresponding to λ. Hence, one has the following equality of functions on $S(n)$:

$$\delta_e = \sum_{\lambda\in\mathbb{Y}_n} \frac{\dim^2\lambda}{n!}\,\frac{\chi^\lambda}{\dim\lambda},$$

where δ_e is the delta-function at the unity, and χ^λ is the irreducible character corresponding to λ.

Let $S(\infty)=\cup_{n\geq 1}S(n)$ be the group of finite permutations of a countable set known as the *infinite symmetric group*, see e.g. [17]. The group $S(\infty)$ has a rich

theory of characters (positive-definite central functions on the group). For any character χ of $S(\infty)$ normalized by $\chi(e)=1$, its restriction to the subgroup $S(n)$ of permutations of first n symbols is a convex combination of $\{\chi^\lambda/\dim\lambda\}_{\lambda\in\mathbb{Y}_n}$. The coefficients $\hat{\chi}_n(\lambda)$ form a probability measure on $\mathbb{Y}_n$; they are a kind of Fourier transform of χ.

There exists only one character χ of $S(\infty)$ for which the rows and columns of the Young diagrams distributed according to $\hat{\chi}_n$ grow sublinearly in n as $n\to\infty$. This character is the delta-function at the unity of $S(\infty)$, the corresponding representation is the (bi)regular representation of $S(\infty)$ in $\ell^2(S(\infty))$, and $\hat{\chi}_n$ is the Plancherel measure on $\mathbb{Y}_n$ introduced above.

An analogous construction for the *infinite–dimensional unitary group* $U(\infty)=\cup_{N\geq 1}U(N)$ yields a two-dimensional family of characters of $U(\infty)$. Although the notion of regular representation for $U(\infty)$ is meaningless, by comparing the lists of the *extreme* (i.e., indecomposable) characters of $S(\infty)$ and $U(\infty)$ one sees that the analog of δ_e on $S(\infty)$ is the family of characters

$$\chi^{\gamma^+,\gamma^-}(U)=\exp\left(\operatorname{Tr}\left(\gamma^+(U-1)+\gamma^-(U^{-1}-1)\right)\right),\qquad U\in U(\infty),$$

where $\gamma^\pm\geq 0$ are the parameters of the family. We will provide details in Section 3, and for now let us just say that on the level of Fourier transform, the set $\mathbb{Y}_n$ is replaced by the set of N-tuples of integers $\lambda_1\geq\cdots\geq\lambda_N$ which we call *signatures* or *highest weights* of length N (they parameterize irreducible representations of the unitary group $U(N)$), and the corresponding probability distributions have the form

$$P_N^{\gamma^+,\gamma^-}(\lambda_1,\dots,\lambda_N)=\operatorname{const}\cdot\det\left[f_i^{(\gamma^+,\gamma^-)}(\lambda_j-j)\right]_{i,j=1}^N\dim_{U(N)}(\lambda),$$

$$f_k^{(\gamma^+,\gamma^-)}(x)=\frac{1}{2\pi i}\oint_{|z|=1}\frac{e^{\gamma^+z+\gamma^-z^{-1}}dz}{z^{x+k+1}},\qquad k=1,2,\dots,$$

where $\dim_{U(N)}(\lambda)$ is the dimension of the irreducible representation of $U(N)$ with highest weight λ. We call the measures $P_N^{\gamma^+,\gamma^-}$ *the Plancherel measures for the infinite-dimensional unitary group*, and the present paper is devoted to the study of these measures.

One source of interest to the Plancherel measures for symmetric groups is the fact that the distribution of the largest part of $\lambda\in\mathbb{Y}_n$ coincides with the distribution of the longest increasing subsequence of uniformly distributed permutation in $S(n)$. This fact can be restated in terms of a random growth model in one space dimension called the polynuclear growth process (PNG). Namely, the distribution of the height function for PNG with the so-called droplet initial condition at any given point in space-time coincides with the distribution of the largest part of $\lambda\in\cup_{n\geq 0}\mathbb{Y}_n$ distributed according to the *Poissonized* Plancherel measure

$$\operatorname{Prob}\{\lambda\}=e^{-\theta^2}\left(\frac{\theta^{|\lambda|}\dim\lambda}{|\lambda|!}\right)^2,\qquad\lambda\in\cup_{n\geq 0}\mathbb{Y}_n,$$

where $|\lambda|$ is the number of boxes in the Young diagram λ, and $\theta > 0$ is a parameter, see [26].

Quite similarly, the largest coordinate of a signature distributed according to the Plancherel measure for $U(\infty)$ describes the height function in another growth model in one space dimension called PushASEP for the so-called step initial condition. This fact can be established by direct comparison of Proposition 3.4 from [6] and Theorem 3.2 below.

The asymptotics of the Plancherel measure for $S(n)$ as $n \to \infty$ has been extensively studied. In the seventies, Logan and Shepp [19] and, independently, Vershik and Kerov [28], [30], discovered that Plancherel distributed Young diagrams have a *limit shape*: In a suitable metric, the measure on these Young diagrams scaled by $\sqrt{n}$ converges as $n \to \infty$ to the delta-measure supported on a certain shape. In the late nineties, more refined results were obtained. It was shown that the random point process generated by the rows (or columns) of the Plancherel distributed Young diagrams has two types of scaling limits, in the "bulk" and at the "edge" of the limit shape. In the limit, the former case yields the discrete sine determinantal point process, while the latter case yields the Airy determinantal point process, see [3], [2], [21], [8], [16].

The main goal of the present paper is to prove similar asymptotics results on scaling limits of random point processes related to more complex measures $P_N^{\gamma^+,\gamma^-}$ with $N \to \infty$ and $\gamma^\pm$ possibly dependent on N. Note that our results do not imply the existence of the limit shape in any of the cases we consider, although they strongly suggest that in some cases the limit shape does exist, and they predict what it looks like. For a discussion of the relationship between "local" results on point processes and "global" measure concentration properties see Remark 1.7 of [8], §1 of [12].

Let us describe our results in more detail.

It is convenient to represent a signature $\lambda = \{\lambda_1 \geq \cdots \geq \lambda_N\}$ as a pair of partitions, one partition λ^+ consists of positive parts of λ while the other one λ^- consists of absolute values of negative parts of λ. When the parameters $\gamma^\pm$ are independent of N, they describe (see Section 2) the asymptotic behavior of $|\lambda^\pm|$, namely $|\lambda^\pm| \sim \gamma^\pm N$, as $N \to \infty$. This asymptotic relation remains true in other situations as well, and it is helpful to keep it in mind when going through the limit transitions below.

Our first result describes what happens when $\gamma^\pm \sim N^{-1}$ as $N \to \infty$. Then one expects that $|\lambda^+|$, $|\lambda^-|$ remain finite in the limit, and indeed the measures $P_N^{(\gamma^+,\gamma^-)}$ converge to the product of two independent copies of the Poissonized Plancherel measures for the symmetric groups that live on $\lambda^\pm$.

The next possibility to consider is when $\gamma^\pm$ are independent of N. The case when $\gamma^- = 0$ was considered by Kerov [18], who proved the existence of the limit shape and showed that the limit shape coincides with that for the Plancherel measures for symmetric groups. We show that when both parameters $\gamma^\pm$ are fixed and nonzero, the random point processes describing $\lambda^\pm$ asymptotically behave as though $\lambda^\pm$ represent two independent copies of the Poissonized Plancherel measures for the symmetric group with Poissonization parameters

$\gamma^{\pm} N \to \infty$.

The most interesting case is when $\gamma^{\pm}$ grow at the same rate as N. Biane [4] proved that when $\gamma^{-} = 0$, the corresponding measure has a limit shape that depends on the limiting value of the ratio γ^{+}/N. We consider the case when both parameters are nonzero and investigate the asymptotic behavior of the random point process that describes our random signatures.

Even though we do not prove the existence of the limit shape, it is convenient to use the hypothetical limit shape inferred from the limit of the density function to describe the results. There are three possibilities: The limit shapes of $\lambda^{\pm}$ scaled by N do not touch (that happens when $\gamma^{\pm}/N$ are small), when they barely meet, and when they have already met, see Figure 4 in the body of the paper. Accordingly, there are three types of local behavior one can expect: The bulk, the edge, where the limit shape becomes tangent to one of the axes, and the point when the edges of the limit shapes for $\lambda^{\pm}$ meet. We compute the local scaling limits of the correlation functions for the random point process describing our signatures, and obtain the correlation functions of the discrete sine, Airy, and Pearcey determinantal processes in the three cases above.

As a matter of fact, we consider probability measures on a more general object than signatures. Every character of $U(\infty)$ naturally defines a probability measure on Gelfand-Tsetlin schemes (a kind of infinite semistandard Young tableaux), see Section 2 and references therein. The corresponding measures on signatures of length N are certain projections of the measure on Gelfand-Tsetlin schemes. In particular, every character from our two-dimensional Plancherel family yields a measure on Gelfand-Tsetlin schemes, and that is what we study asymptotically. We interpret each scheme as a point configuration in $\mathbb{Z}\times\mathbb{Z}_+$, and compute the scaling limits of correlation functions of the arising two-dimensional random point processes. The results are appropriate (determinantal) time-dependent extensions of the limiting processes mentioned above.

The proofs are based on the techniques of determinantal point processes.

First, we show that for any extreme character of $U(\infty)$, the corresponding random point process on $\mathbb{Z} \times \mathbb{Z}_+$ is determinantal, and we compute the correlation kernel in the form of a double contour integral of a fairly simple integrand. This result (Theorem 3.2) is similar in spirit to the formula for the correlation kernel of the Schur process from [23], but it does not seem to be in direct relationship with it. After that we perform the asymptotic analysis of the contour integrals largely following the ideas of [20], [23], [24].

Acknowledgements. The authors are very grateful to Grigori Olshanski for a number of valuable suggestions. The first named author (A. B.) was partially supported by the NSF grant DMS-0707163.

2 Description of the Model

Let $U(N)$ denote the group of all $N \times N$ unitary matrices. For each N, $U(N)$ is naturally embedded in $U(N+1)$ as the subgroup fixing the $(N+1)$-th basis

vector. Equivalently, each $U \in U(N)$ can be thought of as an $(N+1)\times(N+1)$ matrix by setting $U_{i,N+1} = U_{N+1,j} = 0$ for $1 \le i,j \le N$ and $U_{N+1,N+1} = 1$. The union $\cup_{N=1}^{\infty} U(N)$ is denoted $U(\infty)$.

A *character* of $U(\infty)$ is a positive definite function $\chi : U(\infty) \to \mathbb{C}$ which is constant on conjugacy classes and normalized ($\chi(e) = 1$). We further assume that χ is continuous on each $U(N) \subset U(\infty)$. The set of all characters of $U(\infty)$ is convex, and the extreme points of this set are called *extreme characters*.

The extreme characters of $U(\infty)$ can be parametrized as follows: Let $\mathbb{R}^\infty$ denote the product of countably many copies of $\mathbb{R}$. Let Ω be the set of all $(\alpha^+, \alpha^-, \beta^+, \beta^-, \delta^+, \delta^-)$ such that ([25], §1)

$$\alpha^\pm = (\alpha_1^\pm \ge \alpha_2^\pm \ge \ldots \ge 0) \in \mathbb{R}^\infty, \quad \beta^\pm = (\beta_1^\pm \ge \beta_2^\pm \ge \ldots \ge 0) \in \mathbb{R}^\infty, \quad \delta^\pm \in \mathbb{R},$$

$$\sum_{i=1}^{\infty} (\alpha_i^\pm + \beta_i^\pm) \le \delta^\pm, \quad \beta_1^+ + \beta_1^- \le 1.$$

Set

$$\gamma^\pm = \delta^\pm - \sum_{i=1}^{\infty} (\alpha_i^\pm + \beta_i^\pm) \ge 0.$$

Each ω in this set defines a function χ^ω on $U(\infty)$ by

$$\chi^\omega(U) = \prod_{u \in \mathrm{Spectrum}(U)} f_0(u)$$

$$f_0(u) = e^{\gamma^+(u-1)+\gamma^-(u^{-1}-1)} \prod_{i=1}^{\infty} \frac{1+\beta_i^+(u-1)}{1-\alpha_i^+(u-1)} \frac{1+\beta_i^-(u^{-1}-1)}{1-\alpha_i^-(u^{-1}-1)}. \qquad (1)$$

As ω ranges over Ω, the functions χ^ω turn out to be all the extreme characters of $U(\infty)$ ([31], [29], [22]).

Equipping $\mathbb{R}^\infty \times \mathbb{R}^\infty \times \mathbb{R}^\infty \times \mathbb{R}^\infty \times \mathbb{R} \times \mathbb{R}$ with the product topology induces a topology on Ω. For any fixed $U \in U(\infty)$, $\chi^\omega(U)$ is a continuous function of ω. For any character χ of $U(\infty)$, there exists a unique Borel probability measure P on Ω such that

$$\chi(U) = \int_\Omega \chi^\omega(U) dP,$$

see [25], Theorem 9.1. This measure is called the *spectral measure* of χ.

It is a classical result that the irreducible representations of $U(N)$ can be paramterized by nonincreasing sequences $\lambda = (\lambda_1 \ge \ldots \ge \lambda_N)$ of N integers (see e.g. [32]). Such sequences are called *signatures (or highest weights) of length N*. Thus there is a natural bijection $\lambda \leftrightarrow \chi^\lambda$ between signatures of length N and the conventional irreducible characters of $U(N)$.

The extreme characters of $U(\infty)$ can be approximated by χ^λ with growing signatures λ. To state this precisely we need more notation.

Represent a signature λ as a pair of Young diagrams (λ^+, λ^-), where λ^+ consists of positive λ_i's and λ^- consists of negative λ_i's. Zeroes can go in either of the two:

$$\lambda = (\lambda_1^+, \lambda_2^+, \dots, -\lambda_2^-, -\lambda_1^-).$$

Let $d(\cdot)$ denote the number of diagonal boxes of a Young diagram and set $d^+ = d(\lambda^+)$ and $d^- = d(\lambda^-)$. Recall that the Frobenius coordinates p_i, q_i of a Young diagram λ are defined by

$$p_i = \lambda_i - i, \quad q_i = (\lambda')_i - i, \quad 1 \le i \le d(\lambda),$$

where λ' is the transposed diagram.

The dimension of the irreducible representation of $U(N)$ indexed by a signature $\lambda = (\lambda_1, \dots, \lambda_N)$ is given by Weyl's formula:

$$\dim_N \lambda = \chi^\lambda(1, \dots, 1) = \prod_{1 \le i < j \le N} \frac{\lambda_i - i - \lambda_j + j}{j - i}.$$

Define the *normalized* irreducible characters by

$$\tilde{\chi}^\lambda = \frac{1}{\dim_N \lambda} \chi^\lambda.$$

Note that $\tilde{\chi}^\lambda(e) = 1$.

Given a sequence $\{f_N\}$ of functions on $U(N)$, we say that f_N's *approximate* a function f on $U(\infty)$ if for any fixed N_0, the restrictions of the functions f_N (for $N \ge N_0$) to $U(N_0)$ uniformly tend, as $N \to \infty$, to the restriction of f to $U(N_0)$. We have the following approximation theorem:

Theorem 2.1. *Let χ be the extreme character corresponding to $(\alpha^\pm, \beta^\pm, \gamma^\pm) \in \Omega$. Let $\{\lambda(n)\}$ be a sequence of signatures of length n with Frobenius coordinates $p_i^\pm(n), q_i^\pm(n)$. Then the functions $\tilde{\chi}^{\lambda(n)}$ approximate χ iff*

$$\lim_{n\to\infty} \frac{p_i^\pm(n)}{n} = \alpha_i^\pm, \quad \lim_{n\to\infty} \frac{q_i^\pm(n)}{n} = \beta_i^\pm, \quad \lim_{n\to\infty} \frac{|(\lambda(n))^\pm|}{n} = \delta^\pm$$

for all i.

Proof. This theorem is due to Vershik and Kerov [29]. See [22] for a detailed proof. □

Let $\mathbb{GT}_N$ be the set of all signatures of length N and set $\mathbb{GT} = \cup_N \mathbb{GT}_N$. Turn $\mathbb{GT}$ into a graph by drawing an edge between signatures $\lambda \in \mathbb{GT}_N$ and $\mu \in \mathbb{GT}_{N+1}$ if λ and μ satisfy the branching relation $\lambda \prec \mu$, where $\lambda \prec \mu$ means that $\mu_1 \le \lambda_1 \le \mu_2 \le \lambda_2 \le \ldots \le \lambda_N \le \mu_{N+1}$. $\mathbb{GT}$ is also known as the *Gelfand-Tsetlin graph*.

Each character of $U(\infty)$ defines a probability measure P_N on $\mathbb{GT}_N$. If we restrict the extreme character χ^ω to $U(N)$, we can write

$$\chi^\omega|_{U(N)} = \sum_{\lambda \in \mathbb{GT}_N} P_N(\lambda)\tilde{\chi}^\lambda. \tag{2}$$

Definition 2.2. *The measure P_N corresponding to the extreme character with $\alpha^\pm = \beta^\pm = 0$ and arbitrary $\gamma^\pm \geq 0$ will be called the Nth level Plancherel measure with parameters $\gamma^\pm$. Denote it by $P_N^{\gamma^+,\gamma^-}$.*

The choice of the term is explained by the analogy with the infinite symmetric group $S(\infty)$. The extreme characters of $S(\infty)$ are parameterized by

$$\{(\alpha,\beta,\gamma) \in \mathbb{R}_+^\infty \times \mathbb{R}_+^\infty \times \mathbb{R}_+; \sum(\alpha_i+\beta_i)+\gamma = 1\}.$$

The measure on partitions of n obtained from the character with $\alpha_i = \beta_i = 0, \gamma = 1$, simiarly to the measure P_N above, assigns the weight $(\dim\lambda)^2/n!$ to a partition λ and is commonly called the Plancherel measure. Here $\dim\lambda$ is the dimension of the irreducible representation of S_n corresponding to λ.

Let χ be a character of $U(\infty)$ and let P and P_N be its corresponding decomposing measures on Ω and $\mathbb{GT}_N$. For any N, embed $\mathbb{GT}_N$ into Ω by sending λ to $(a^+, a^-, b^+, b^-, c^+, c^-)$ where

$$a_i^\pm = \frac{p_i^\pm}{N}, \quad b_i^\pm = \frac{q_i^\pm}{N}, \quad c^\pm = \frac{|\lambda^\pm|}{N}.$$

Define a probability measure $\underline{P}_N$ on Ω to be the pushforward of P_N under this embedding. Then $\underline{P}_N$ weakly converges to P as $N \to \infty$ ([25], Theorem 10.2).

This implies that as $N \to \infty$, the Plancherel measures $P_N^{\gamma^+,\gamma^-}$ converge to the delta measure at $\omega = (\alpha_i^\pm = \beta_i^\pm = 0, \gamma^+, \gamma^-)$, that is, the row and column lengths for $\lambda^\pm$ distributed according to $P_N^{\gamma^+,\gamma^-}$ grow sublinearly in N.

The main goal of this paper is to study the asymptotic behavior of the signatures distributed according to the Plancherel measures $P_N^{\gamma^+,\gamma^-}$ as $N \to \infty$. We will also study a more general object: the corresponding probability measures on objects called paths in $\mathbb{GT}$.

A *path* in $\mathbb{GT}$ is an infinite sequence $t = (t_1, t_2, \ldots)$ such that $t_i \in \mathbb{GT}_i$ and $t_i \prec t_{i+1}$. Let $\mathcal{T}$ be the set of all paths.

We also have *finite paths*, which are sequences $\tau = (\tau_1, \tau_2, \ldots, \tau_N)$ such that $\tau_i \in \mathbb{GT}_i$ and $\tau_1 \prec \tau_2 \prec \ldots \prec \tau_N$. The set of all paths of length N is denoted by $\mathcal{T}_N$. For each finite path $\tau \in \mathcal{T}_N$, let C_τ be the cylinder set

$$C_\tau = \{t \in \mathcal{T} \colon (t_1, t_2, \ldots, t_N) = \tau\}.$$

A character χ of $U(\infty)$ also defines a probability measure M^χ on $\mathcal{T}$ which can be specified by setting

$$M^\chi(C_\tau) = \frac{P_N(\lambda)}{\dim_N \lambda}, \tag{3}$$

where P_N is as above and τ is an arbitrary finite path ending at λ ([25],§10). In particular, any $\omega \in \Omega$ defines a measure on $\mathcal{T}$ via the corresponding extreme character χ^ω. If ω satisfies $\alpha_i^\pm = \beta_i^\pm = 0$ with arbitrary $\gamma^\pm$, then let P^{γ^+,γ^-} denote this measure.

3 Plancherel measures as determinantal point processes

In order to analyze $P_N^{\gamma^+,\gamma^-}$ and P^{γ^+,γ^-}, it is convenient to represent signatures as finite point configurations (subsets) in one-dimensional lattice. Assign to each signature $\lambda \in \mathbb{GT}_N$ a point configuration $\mathcal{L}(\lambda) \subset \mathbb{Z}$ by

$$\lambda = (\lambda_1, \dots, \lambda_N) \mapsto \mathcal{L}(\lambda) = \{\lambda_1 - 1, \dots, \lambda_N - N\}.$$

The pushforward of $P_N^{\gamma^+,\gamma^-}$ under this map is a measure on subsets of $\mathbb{Z}$, that is, a random point process on $\mathbb{Z}$. Denote this point process by $\mathcal{P}_N^{\gamma^+,\gamma^-}$. The map $\lambda \mapsto \mathcal{L}(\lambda)$ can be seen visually. For example, if $\lambda = (4, 2, 0, 0, -1, -3)$, then $\mathcal{L}(\lambda) = \{3, 0, -3, -4, -6, -9\}$. See Figure 1.

Figure 1: Black dots represent points in the configuration and white dots represent points not in the configuration.

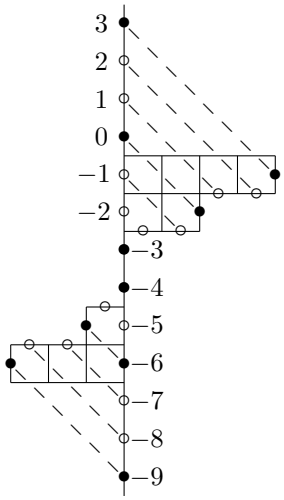

Given a point process on $\mathbb{Z}$, define the *nth correlation function* ρ_n by

$$\rho_n : \mathbb{Z}^n \to [0, 1]$$

$$(x_1, x_2, \dots, x_n) \mapsto \text{Prob}(\{X \subset \mathbb{Z} : \{x_1, x_2, \dots, x_n\} \subset X\}).$$

(There is a more general definition of correlation functions, but it will not be needed here. See e.g. [9], §5 for more details). Clearly, this function is symmetric with respect to the permutations of the arguments.

On a countable discrete state space ($\mathbb{Z}$ in our case) a point process is uniquely determined by its correlation functions (see e.g. [5], §4), so to study the measure it suffices to study its correlation functions.

A point process is *determinantal* if there exists a function K such that

$$\rho_n(x_1, x_2, \dots, x_n) = \det[K(x_i, x_j)]_{1 \le i,j \le n} \quad \text{for any } n = 1, 2, \dots.$$

The function K is the *correlation kernel*. A useful observation is that K is not unique: $K(x, y)$ and $\frac{f(x)}{f(y)} K(x, y)$ define the same correlation functions for an arbitrary function f.

Just as $\lambda \mapsto \mathcal{L}(\lambda)$ defines a map from $\mathbb{GT}_n$ to the set of subsets of $\mathbb{Z}$, we have a map from the set $\mathcal{T}$ of paths in the Gelfant-Tsetlin graph to subsets of $\mathbb{Z}_+ \times \mathbb{Z}$. Let $t = (t_1 \prec t_2 \prec \dots)$ be a path in $\mathbb{GT}$. Each t_i is a signature of length i which will be written as $\lambda^{(i)} = (\lambda_1^{(i)}, \lambda_2^{(i)}, \dots, \lambda_i^{(i)})$. Then map t to

$$\mathcal{L}(t) = \{(i, \lambda_j^{(i)} - j) : 1 \le i < \infty, 1 \le j \le i\} \subset \mathbb{Z}_+ \times \mathbb{Z}.$$

The pushforward of P^{γ^+, γ^-} under this map will be denoted by $\mathcal{P}^{\gamma^+, \gamma^-}$. This is a random point process on $\mathbb{Z}_+ \times \mathbb{Z}$.

One more introductory concept is needed. Define a map Δ by

$$\Delta : 2^{\mathbb{Z}_+ \times \mathbb{Z}} \to 2^{\mathbb{Z}_+ \times \mathbb{Z}}, \quad X \mapsto (\mathbb{Z}_+ \times \mathbb{Z}) \backslash X.$$

Given a point process $\mathcal{P}$ on $\mathbb{Z}_+ \times \mathbb{Z}$, its pushforward under Δ is also a point process on $\mathbb{Z}_+ \times \mathbb{Z}$, which will be denoted $\mathcal{P}_\Delta$. The map Δ is often referred to as "particle-hole involution". With this notation, we have the following proposition:

Proposition 3.1. *If $\mathcal{P}$ is a determinantal point process with correlation kernel $K(n_i, x_i; n_j, x_j)$, then $\mathcal{P}_\Delta$ is also a determinantal point prcess. Its correlation kernel is $\delta_{n_i = n_j, x_i = x_j} - K(n_i, x_i; n_j, x_j)$.*

Proof. See Proposition A.8 of [8]. □

Let us now state the main theorem of this section.

Theorem 3.2. *The point process $\mathcal{P}^{\gamma^+, \gamma^-}$ is determinantal. Let $K(n_i, x_i; n_j, x_j)$ denote its correlation kernel. If $n_1 \ge n_2$, then*

$$K(n_1, x_1; n_2, x_2) = \left(\frac{1}{2\pi i}\right)^2 \oint \oint \frac{e^{\gamma^- u + \gamma^+ u^{-1}} u^{x_1} (1-u)^{n_1}}{e^{\gamma^- w + \gamma^+ w^{-1}} w^{1+x_2} (1-w)^{n_2}} \frac{du dw}{u - w}.$$

If $n_1 < n_2$, then

$$K(n_1, x_1; n_2, x_2) = -\frac{1}{2\pi i} \oint \frac{z^{x_1 - x_2 - 1}}{(1-z)^{n_2 - n_1}} dz + \left(\frac{1}{2\pi i}\right)^2 \oint \oint \frac{e^{\gamma^- u + \gamma^+ u^{-1}} u^{x_1} (1-u)^{n_1}}{e^{\gamma^- w + \gamma^+ w^{-1}} w^{1+x_2} (1-w)^{n_2}} \frac{du dw}{u - w}. \quad (4)$$

In these expressions, u is integrated over $|u| = r < 1$ and w is integrated over $|w-1| = \epsilon < 1 - r$ and z is integrated over $|z| = r < 1$.

Corollary 3.3. *The point process $\mathcal{P}_{\Delta}^{\gamma^+,\gamma^-}$ is determinantal. Let $K_{\Delta}(n_i, x_i; n_j, x_j)$ denote its correlation kernel. If $n_1 > n_2$, then*

$$K_{\Delta}(n_1, x_1; n_2, x_2) = -\left(\frac{1}{2\pi i}\right)^2 \oint\oint \frac{e^{\gamma^- u + \gamma^+ u^{-1}} u^{x_1} (1-u)^{n_1}}{e^{\gamma^- w + \gamma^+ w^{-1}} w^{1+x_2} (1-w)^{n_2}} \frac{du dw}{u-w}.$$

If $n_1 \le n_2$, then

$$K_{\Delta}(n_1, x_1; n_2, x_2) = \frac{1}{2\pi i} \oint \frac{z^{x_1 - x_2 - 1}}{(1-z)^{n_2 - n_1}} dz - \left(\frac{1}{2\pi i}\right)^2 \oint\oint \frac{e^{\gamma^- u + \gamma^+ u^{-1}} u^{x_1} (1-u)^{n_1}}{e^{\gamma^- w + \gamma^+ w^{-1}} w^{1+x_2} (1-w)^{n_2}} \frac{du dw}{u-w}. \quad (5)$$

In these expressions, u is integrated over $|u| = r < 1$ and w is integrated over $|w-1| = \epsilon < 1 - r$ and z is integrated over $|z| = r < 1$.

Proof. The corollary follows immediately from Proposition 3.1 and the fact that

$$\delta_{x_1 = x_2} = \frac{1}{2\pi i} \oint_{|z|=r} \frac{z^{x_1 - x_2 - 1}}{(1-z)^{n_2 - n_1}} dz$$

for $n_1 = n_2$. Note that in Theorem 3.2 the two cases for the kernel are $n_1 \ge n_2$ and $n_1 < n_2$, while in Corollary 3.3 the two cases are $n_1 > n_2$ and $n_1 \le n_2$. □

Remark. Let $\bar{K}(n_1, x_1; n_2, x_2)$ and $\bar{K}_{\Delta}(n_1, x_1; n_2, x_2)$ denote the correlation kernels of $\mathcal{P}^{\gamma^-,\gamma^+}$ and $\mathcal{P}_{\Delta}^{\gamma^-,\gamma^+}$, respectively ($\gamma^+$ and γ^- switched places). The substitutions $u \mapsto u^{-1}, w \mapsto w^{-1}$ and further deformation of the contours show that

$$(-1)^{n_1 - n_2} K(n_1, -x_1 - n_1 - 1; n_2, -x_2 - n_2 - 1) = \bar{K}(n_1, x_1; n_2, x_2),$$

$$(-1)^{n_1 - n_2} K_{\Delta}(n_1, -x_1 - n_1 - 1; n_2, -x_2 - n_2 - 1) = \bar{K}_{\Delta}(n_1, x_1; n_2, x_2).$$

This can be understood independently. Switching γ^+ and γ^- corresponds to switching λ^+ and λ^- in a signature λ. In terms of $\mathcal{L}(\lambda)$, this corresponds to replacing x_i with $-x_i - n_i - 1$. For example, consider $\lambda = (4, 2, 0, 0, -1, -3)$ from Figure 1. Switching λ^+ and λ^- gives $\bar{\lambda} = (3, 1, 0, 0, -2, -4)$. Then $\mathcal{L}(\bar{\lambda}) = \{2, -1, -3, -4, -7, -10\}$, which can be obtained from $\mathcal{L}(\lambda)$ by replacing x_i with $-x_i - 6 - 1$.

Remark. The arguments below actually prove a more general statement. If we define a point process of $\mathbb{Z}_+ \times \mathbb{Z}$ similarly to $\mathcal{P}^{\gamma^+,\gamma^-}$, but starting from an extreme character of $U(\infty)$ with arbitrary parameters $(\alpha_i^{\pm}, \beta_i^{\pm}, \gamma^{\pm})$, then this process is determinantal and its kernel has a similar form. The only change is replacing $E(z)$ below by $f_0(z)$ from equation (1).

In what follows we use the notation

$$E(z) = e^{\gamma^+(z-1) + \gamma^-(z^{-1}-1)} = e^{-\gamma^+ - \gamma^-} e^{\gamma^+ z + \gamma^- z^{-1}}.$$

Lemma 3.4. *Suppose $\lambda = (\lambda_1, \lambda_2, \ldots, \lambda_N) \in \mathbb{GT}_N$. Write x_k for $\lambda_k - k$. Then*

$$P_N^{\gamma^+,\gamma^-}(\lambda) = \text{const} \cdot \det[f_j(x_k)]_{1\le j,k\le N} \det[g_j(x_k)]_{1\le j,k\le N}$$

where

$$f_j(x_k) = \frac{1}{2\pi i}\oint_{|u|=1} E(u)u^{-1-x_k-j}du, \qquad 1 \le j \le N. \tag{6}$$

$$g_j(x_k) = x_k^{j-1}, \qquad 1 \le j \le N. \tag{7}$$

Proof. Writing $E(u) = \sum_{l=-\infty}^{\infty} c(l)u^l$ and integrating $E(u)u^k$ over the unit circle, we can solve for c to get

$$c(l) = \frac{1}{2\pi i}\oint_{|u|=1} E(u)u^{-1-l}du$$

Set $\omega = (\alpha_i^{\pm} = \beta_i^{\pm} = 0, \gamma^+, \gamma^-)$. For $U \in U(N)$ with spectrum $u_1, \ldots, u_N$, we can write $\chi^\omega(U) = E(u_1)\ldots E(u_N)$. Recall that $P_N^{\gamma^+,\gamma^-}$ is defined by (2). Using ([25], Lemma 6.5), we can express $\chi^\omega|_{U(N)}$ as $\sum_{\lambda\in\mathbb{GT}_N} c(\lambda)\chi^\lambda$, where

$$c(\lambda) = c(\lambda_1, \ldots, \lambda_N) = \det[c(\lambda_k - k + j)]_{1\le j,k\le N}.$$

Set $f_j(x_k) = c(x_k + j)$. Since $\chi^\lambda = \tilde{\chi}^\lambda \cdot \dim_N \lambda$, with

$$\dim_N \lambda = \prod_{1\le i<j\le N} \frac{\lambda_i - i - \lambda_j + j}{j - i} = \text{const} \cdot \prod_{1\le i<j\le N} ((\lambda_i - i) - (\lambda_j - j)),$$

we get the additional Vandermonde determinant $\det[(\lambda_k - k)^{j-1}] = \det[x_k^{j-1}]$. □

Remark. Observe that the argument above and (3) imply that $P^{\gamma^+,\gamma^-}(C_\tau) = \det[f_j(x_k)]_{1\le j,k\le N}$.

To state the next result we need slightly different notation. Let

$$\mathcal{P}^{\gamma^+,\gamma^-}(\{x_k^{(n)} : 1 \le n \le N,\ 1 \le k \le n\}) = P^{\gamma^+,\gamma^-}(C_\tau)$$

if there exists a path $\tau = (\lambda^{(1)} \prec \ldots \prec \lambda^{(n)})$ such that

$$\lambda^{(n)} = (x_1^{(n)} + 1, x_2^{(n)} + 2, \ldots, x_n^{(n)} + n),$$

and $\mathcal{P}^{\gamma^+,\gamma^-}(\{x_k^{(n)}\}) = 0$ otherwise.

Proposition 3.5. *Let $\{x_k^{(n)} : 1 \le n \le N, 1 \le k \le n\}$ be arbitrary integers satisfying $x_k^{(n)} \ge x_{k+1}^{(n)}$ for all n, k. Then*

$$\mathcal{P}^{\gamma^+,\gamma^-}(\{x_k^{(n)} : 1 \le n \le N,\ 1 \le k \le n\}) =$$
$$\text{const} \cdot \prod_{n=1}^{N-1} \det[\phi_n(x_i^{(n)}, x_j^{(n+1)})]_{1 \le i,j \le n+1} \det[f_i(x_j^{(N)})]_{1 \le i,j \le N}$$

where $x_{n+1}^{(n)}$ are virtual variables[1]*, and ϕ_n is defined by*

$$\phi_n(x,y) := \begin{cases} 1 & \text{if } x \le y, \\ 1 & x \text{ virtual}, \\ 0 & \text{otherwise.} \end{cases}$$

Proof. By the remark after 3.4, it suffices to prove that $\prod \det[\phi_n]$ acts as a indicator function. It takes the value of 1 if $\lambda^{(1)} \prec \lambda^{(2)} \prec \ldots \prec \lambda^{(N)}$ and 0 otherwise, where

$$\lambda^{(n)} = (x_1^{(n)} + 1, \ldots, x_n^{(n)} + n).$$

If $\lambda^{(1)} \prec \lambda^{(2)} \prec \ldots \prec \lambda^{(N)}$, so that $x_1^{(n+1)} \ge x_1^{(n)} > x_2^{(n+1)} \ge x_2^{(n)} > \ldots \ge x_n^{(n)} > x_{n+1}^{(n+1)}$ for each n, then

$$\phi_n(x_i^{(n)}, x_j^{(n+1)}) = \begin{cases} 1 & \text{if } j \le i, \\ 0 & \text{if } i < j. \end{cases}$$

So $\det[\phi_n] = 1$ for each n.

Conversely, suppose that $\prod \det[\phi_n] = 1$, so that $\det[\phi_n] \neq 0$ for each n. Notice that the matrix $[\phi_n(x_i^{(n)}, x_j^{(n+1)})]$ consists entirely of zeroes and ones. Also notice that the number of ones in the kth column is greater than or equal to the number of ones in the jth column for $k < j$. Additionally, if the (i,j) entry is zero then so is the $(i-1,j)$ entry. Since the determinant is nonzero, this means that no two columns are equal, so each column must have a different number of ones, so the (i,j) entry is 1 if $j \le i$ and 0 if $i < j$. This says exactly that $\lambda^{(1)} \prec \lambda^{(2)} \prec \ldots \prec \lambda^{(N)}$, and each determinant in the product is equal to 1. □

We can now prove Theorem 3.2.

Proof of Theorem 3.2. For computational purposes, it is actually easier to consider

$$\phi_n(x,y) := \begin{cases} \theta_n^{x-y} & \text{if } x \le y, \\ \theta_n^{-y} & x \text{ virtual}, \\ 0 & \text{otherwise.} \end{cases}$$

with mutually distinct θ_n's and then take $\theta_n \to 1$. It is also convenient to denote $\theta_0 = 1$. We will assume that $|\theta_n| > |\theta_{n-1}| > 1$ for all n. Notice that $\det[f_i(x_j^{(N)})]$ only depends on the linear span of $f_1, \ldots, f_N$ (up to a constant), so redefine

[1] One can think of virtual variables as being equal to negative infinity.

$$f_j(x) = \frac{1}{2\pi i} \oint_{|u|=const} E(u) u^{-2-x} p_{j-1}(u^{-1}) du, \text{ where}$$

$$p_{j-1}(x) = (\theta_0 - x) \dots (\widehat{\theta_{j-1} - x}) \dots (\theta_{N-1} - x) = \prod_{k=0, k\neq j-1}^{N-1} (\theta_k - x).$$

The rest of the proof is a direct application of Lemma 3.4 of [7], where we use the notation $\Psi^N_{N-j} = f_j$.

Taking the Fourier Transform of ϕ_n, we obtain

$$\phi_n(x,y) = \frac{1}{2\pi i} \oint_{|z|=1} F_n(z) z^{x-y-1} dz$$

$$\phi^{(n_1,n_2)}(x,y) = \frac{1}{2\pi i} \oint_{|z|=1} F_{n_1}(z) \dots F_{n_2-1}(z) z^{x-y-1} dz \tag{8}$$

where $F_n(z) = (1 - \theta_n^{-1} z)^{-1}$ and $n_1 < n_2$. We also agree that $\phi^{(n_1,n_2)} \equiv 0$ if $n_1 \geq n_2$. In case x is a virtual variable (which is denoted by $virt$), then

$$\begin{aligned}
\phi^{(n_1,n_2)}(virt, y) =& \sum_{m\in\mathbb{Z}} \phi_{n_1}(virt, m) \phi^{(n_1+1,n_2)}(m, y) \\
=& \frac{\theta_{n_1}^{-y}}{2\pi i} \oint_{|\theta_{n_1}|<|z|=const<|\theta_{n_1+1}|} F_{n_1+1}(z) \dots F_{n_2-1}(z) \frac{dz}{z - \theta_{n_1}} \\
=& \theta_{n_1}^{-y} F_{n_1+1}(\theta_{n_1}) \dots F_{n_2-1}(\theta_{n_1})
\end{aligned}$$

This allows us to calculate the matrix M (cf. [7], Lemma 3.4). In the following equation, $\Gamma(r_1, r_2)$ denotes the boundary of an annulus of radii $r_1 < r_2$ in the complex plane.

$$\begin{aligned}
M_{ij} =& (\phi^{(i-1,N)} * \Psi^N_{N-j})(virt) = \sum_{y\in\mathbb{Z}} \phi^{(i-1,N)}(virt, y) \Psi^N_{N-j}(y) \\
=& \sum_{y\in\mathbb{Z}} \theta_{i-1}^{-y} F_i(\theta_{i-1}) \dots F_{N-1}(\theta_{i-1}) \cdot \frac{1}{2\pi i} \oint_{|u|=1} E(u) u^{-2-y} p_{j-1}(u^{-1}) du \\
=& - F_i(\theta_{i-1}) \dots F_{N-1}(\theta_{i-1}) \frac{1}{2\pi i} \oint_{\Gamma(r,1), r<|\theta_{i-1}|^{-1}} E(u) u^{-2} p_{j-1}(u^{-1}) \frac{u\theta_{i-1}}{1 - u\theta_{i-1}} du \\
=& F_i(\theta_{i-1}) \dots F_{N-1}(\theta_{i-1}) E(\theta_{i-1}^{-1}) p_{j-1}(\theta_{i-1}) \theta_{i-1}.
\end{aligned}$$

Notice that M is diagonal because $p_{j-1}(\theta_{i-1}) = 0$ unless $i = j$. We have one more preliminary calcuation (cf. [7], formula (3.22)):

$$\begin{aligned}
&\Psi^n_{n-j}(x) = \sum_{y\in\mathbb{Z}} \phi^{(n,N)}(x,y)\Psi^N_{N-j}(y)\\
=&\left(\frac{1}{2\pi i}\right)^2 \oint_{|z|=1} F_n(z)\dots F_{N-1}(z)z^{x-1}dz \oint_{|u|=R>1} E(u)u^{-2}p_{j-1}(u^{-1})\sum_{y\geq x}(zu)^{-y}du\\
=&\left(\frac{1}{2\pi i}\right)^2 \oint_{|z|=1} F_n(z)\dots F_{N-1}(z)z^{-1}dz \oint_{|u|=R>1} E(u)u^{-2-x}p_{j-1}(u^{-1})\frac{du}{1-(zu)^{-1}}\\
=&\frac{1}{2\pi i}\oint_{|u|=1} F_n(u^{-1})\dots F_{N-1}(u^{-1})E(u)u^{-2-x}p_{j-1}(u^{-1})du
\end{aligned}$$

We can now calculate K according to [7], formula (3.26). For $n_1 < n_2$,

$$\begin{aligned}
&K(n_1,x_1;n_2,x_2) + \phi^{(n_1,n_2)}(x_1,x_2)\\
=&\sum_{k=1}^{n_2}[M^{-1}]_{kk}\Psi^{n_1}_{n_1-k}(x_1)\phi^{(k-1,n_2)}(virt,x_2)\\
=&\frac{1}{2\pi i}\oint_{|u|=1} F_{n_1}(u^{-1})\dots F_{N-1}(u^{-1})E(u)u^{-2-x_1}\\
&\quad\times\sum_{k=1}^{n_2}\frac{\theta_{k-1}^{-x_2}F_k(\theta_{k-1})\dots F_{n_2-1}(\theta_{k-1})p_{k-1}(u^{-1})}{F_k(\theta_{k-1})\dots F_{N-1}(\theta_{k-1})E(\theta_{k-1}^{-1})p_{k-1}(\theta_{k-1})\theta_{k-1}}du\\
=&\frac{1}{2\pi i}\oint_{|u|=1} F_{n_1}(u^{-1})\dots F_{N-1}(u^{-1})E(u)u^{-2-x_1}\\
&\quad\times\sum_{k=1}^{n_2}\frac{\theta_{k-1}^{-x_2}p_{k-1}(u^{-1})}{F_{n_2}(\theta_{k-1})\dots F_{N-1}(\theta_{k-1})E(\theta_{k-1}^{-1})p_{k-1}(\theta_{k-1})\theta_{k-1}}du\\
=&\frac{1}{2\pi i}\oint_{|u|=1} u^{-2-x_1}\\
&\quad\times\left(\sum_{k=1}^{n_1}\frac{\theta_{n_1}\dots\theta_{N-1}E(u)\prod_{l=0,l\neq k-1}^{n_1-1}(\theta_l-u^{-1})}{\theta_{n_2}\dots\theta_{N-1}E(\theta_{k-1}^{-1})\prod_{l=0,l\neq k-1}^{n_2-1}(\theta_l-\theta_{k-1})}\theta_{k-1}^{-1-x_2}\right.\\
&\quad\left.+\sum_{k=1+n_1}^{n_2}\frac{\theta_{n_1}\dots\theta_{N-1}E(u)\prod_{l=0}^{n_1-1}(\theta_l-u^{-1})}{(\theta_{k-1}-u^{-1})\theta_{n_2}\dots\theta_{N-1}E(\theta_{k-1})\prod_{l=0,l\neq k-1}^{n_2-1}(\theta_l-\theta_{k-1})}\theta_{k-1}^{-1-x_2}\right)du
\end{aligned}$$

and for $n_1 \geq n_2$ the last sum is omitted.

We can write the expression in parantheses as a contour integral that goes around all the θ_j, so we get

$$\left(\frac{1}{2\pi i}\right)^2 \oint_{|u|=r^{-1}>1}\oint_{|z-1|=\epsilon}\frac{(\theta_0-u^{-1})\dots(\theta_{n_1-1}-u^{-1})E(u)u^{-2-x_1}}{(\theta_0-z)\dots(\theta_{n_2-1}-z)E(z^{-1})z^{1+x_2}}\frac{\theta_{n_2}\dots\theta_{n_1-1}}{(u^{-1}-z)}dudz,$$

assuming that $|\theta_n - 1| < \epsilon$ for all n. Substituting $u \to u^{-1}$ gives

$$\left(\frac{1}{2\pi i}\right)^2 \oint_{|u|=r<1} \oint_{|z-1|=\epsilon} \frac{(\theta_0 - u)\dots(\theta_{n_1-1} - u)E(u^{-1})u^{x_1}}{(\theta_0 - z)\dots(\theta_{n_2-1} - z)E(z^{-1})z^{1+x_2}} \frac{\theta_{n_2}\dots\theta_{n_1-1}}{(u-z)} dudz.$$

There is also the term $-\phi^{(n_1,n_2)}(x_1, x_2)$ from (8), which equals

$$-\left(\frac{1}{2\pi i}\right)^2 \oint_{|z|=const<1} \frac{z^{x_1-x_2-1}}{(1-\theta_{n_1}^{-1}z)\dots(1-\theta_{n_2-1}^{-1}z)} dz$$

if $n_1 < n_2$ and 0 if $n_1 \geq n_2$. Finally, taking all the θ_j to be 1 yields the result.

4 Limits

4.1 Limit Shape

Represent $\lambda \in \mathbb{GT}_N$ as a pair of Young diagrams (λ^+, λ^-). Figure 2 gives an example with $\lambda = (4, 2, 0, 0, -1, -3), \lambda^+ = (4, 2), \lambda^- = (3, 1)$. We have the

Figure 2: The double lines show the boundary.

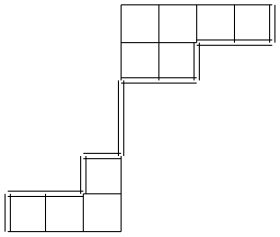

following conjecture:

Regard $\lambda \in \mathbb{GT}_N$ as random objects on the probability space $(\mathbb{GT}_N, P_N^{\gamma^+,\gamma^-})$. As $N \to \infty$, the boundaries of the two Young diagrams, scaled by $N^{-1/2}$, tend to (nonrandom) limit curves. Both limit curves coincide with the limit curve arising from the Plancherel measure on symmetric groups.

Our results strongly suggest that this statement holds, see §3.2.

The conditions $\alpha_i^{\pm} = \beta_i^{\pm} = 0$ tell us that for fixed $\gamma^{\pm}$ every row and column length grows sublinearly in N (see the end of §1). Furthermore, since $\gamma^{\pm}$ correspond to the area of the Young diagrams $\lambda^{\pm}$ (see §1), this suggests a scaling of $N^{-1/2}$. See Figure 3.

Furthermore, we see from Figure 1 that vertical segments of the boundary correspond to points in the configuration, while horizontal segments correspond to points not in the configuration. This implies that the first correlation function $\rho_1(x)$ (also known as the density function) corresponds to the density of vertical segments in the boundary. For example, in between the two curves in Figure 3,

Figure 3: A visual representation

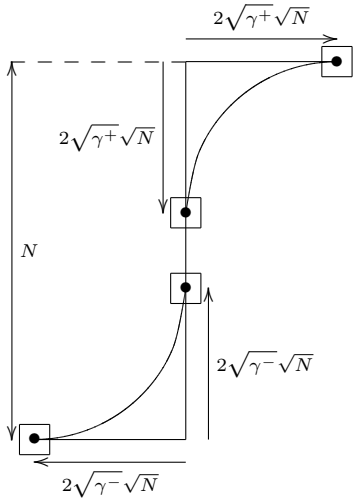

the vertical segments are densely packed, so $\rho_1(x)$ should converge to 1. Above the top curve (the boundary of λ^+) and below the bottom curve (the boundary of λ^-), the horizontal segments are densely packed, so $\rho_1(x)$ should converge to 0. We will see that this is indeed the case.

Notice that near the edges of the Young diagrams (the boxes in Figure 3), the probability of finding a vertical segment tends to 0 or 1. This means that the vertical segments (or horizontal segments) become so rare that they occur infinitely far away from each other. In other words, for any fixed k, the differences $\lambda_k^{\pm} - \lambda_{k+1}^{\pm}$ and $(\lambda^{\pm})'_k - (\lambda^{\pm})'_{k+1}$ both go to infinity as $N \to \infty$. In fact, we find that $\lambda_k^{\pm} - \lambda_{k+1}^{\pm}$ and $(\lambda^{\pm})'_k - (\lambda^{\pm})'_{k+1}$ are of order $N^{1/6}$. The limiting distribution of $\lambda_k^{\pm} - \lambda_{k+1}^{\pm}$ or $(\lambda^{\pm})'_k - (\lambda^{\pm})'_{k+1}$ normalized by $N^{1/6}$ is referred to as the *edge scaling limit*. We will later prove that the well known Airy determinantal point process appears in the edge limits. On the other hand, if we zoom in at any other point on the limit curves, the behavior there is different. At these points, the differences between consecutive rows and columns stay finite. Their limiting distributions are described by the *bulk limit*. We prove that it coincides with the discrete sine determinantal process. The limit density function in the bulk predicts the limit shape.

We should also consider what happens to the more general object – the corresponding measure on the set τ of paths in $\mathbb{GT}$ (see §1). Consider two signatures on such a path at levels n_1 and n_2. If $n_1 - n_2$ stays bounded then the bulk and the edge limits of these two signatures are indistinguishable (the local point configurations are essentially the same). However, as $n_2 - n_1$ grows, we may see nontrivial joint distributions. It turns out that the proper level scaling

in the bulk is $n_1 - n_2 \sim \sqrt{N}$ while at the edge it is $n_1 - n_2 \sim N^{2/3}$. We will compute the corresponding scaling limits of the correlation functions later.

It is also interesting to consider the case when the parameters $\gamma^{\pm}$ depend on N. If $\gamma^{\pm}$ depend on N in such a way that $\gamma^{\pm} N \to a > 0$, then the areas of the Young diagrams $\lambda^{\pm}$ stay finite. More precisely, we obtain two independent copies of the Poissonized Plancherel measure for symmetric groups.

Additionally, consider what happens when $\gamma^{\pm}$ depend on N in such a way that $\gamma^{+}/N \to a > 0$ and $\gamma^{-}/N \to b > 0$ as $N \to \infty$. The Young diagrams are now scaled by N^{-1}. The new hypothetical limit shape depends on the values of a and b. See Figure 4.

The edges of the limit curves correspond to the real roots of a fourth degree polynomial

$$Q_{a,b}(z) = p_0 + p_1 \left(z + \frac{1}{2}\right) + p_2 \left(z + \frac{1}{2}\right)^2 + p_3 \left(z + \frac{1}{2}\right)^3 + 16 \left(z + \frac{1}{2}\right)^4,$$

$$p_0 = 1 - 12(a+b) + 4(a^2+b^2) + 184ab - 256ab(a+b) + 64ab(a-b)^2,$$

$$p_1 = 8(b-a)(7 - 2a - 2b + 16ab),$$

$$p_2 = 8(2(a+b)^2 - 10(a+b) - 1), \quad p_3 = 32(b-a).$$

The expression $Q_{a,b}(c)$ is the discriminant of a simpler polynomial

$$R_{a,b,c}(z) = -bz^3 + (b - c - 1)z^2 + (c + a)z - a.$$

For small a and b, $Q_{a,b}$ has four real roots. As a and b increase, two of the real roots become closer until they merge into a double root. For larger values of a and b, $Q_{a,b}(z)$ has two real roots.

We will be able to find what values of a and b lead to $Q_{a,b}$ having exactly three distinct real roots (the middle root is a double root). This corresponds to the situation when the two limit curves just barely merge (see the middle image in Figure 4). The correct scaling there is to let $(\lambda^{\pm})'_i - (\lambda^{\pm})'_{i+1} \sim N^{1/4}$ and $n_1 - n_2 \sim N^{1/2}$, which results in the Pearcey determinantal process appearing in the limit. At the other edges, letting $\lambda_i - \lambda_{i+1} \sim N^{1/3}$ or $(\lambda^{\pm})'_i - (\lambda^{\pm})'_{i+1}$ and $n_1 - n_2 \sim N^{2/3}$ results in the Airy process appearing. Away from the edges we still observe the bulk limit.

We now proceed to computing the (scaling) limits of our determinantal point process $\mathcal{P}^{\gamma^+,\gamma^-}$ corresponding to the limit regimes described above.

4.2 Limits with $\gamma^{\pm} \propto 1/N$

Introduce the kernel $\mathbb{J}$ on $\mathbb{R}_+ \times \mathbb{Z}$ by

$$\mathbb{J}(s,x;t,y) = \left(\frac{1}{2\pi i}\right)^2 \oint \oint \frac{e^{u^{-1} - tu - w^{-1} + sw}}{w - u} \frac{dudw}{w^{x+1} u^{-y}}$$

where the w and u contours go counterclockwise around 0 in such a way that the w-contour contains the u-contour if $s \geq t$, and the w-contour is contained

Figure 4: The limit curves for various values of a and b. The top curve occurs when $a = \frac{1}{25}, b = \frac{1}{15}$, the middle curve occurs when $a = b = \frac{1}{8}$, the bottom curve occurs when $a = \frac{1}{4}, b = \frac{1}{3}$.

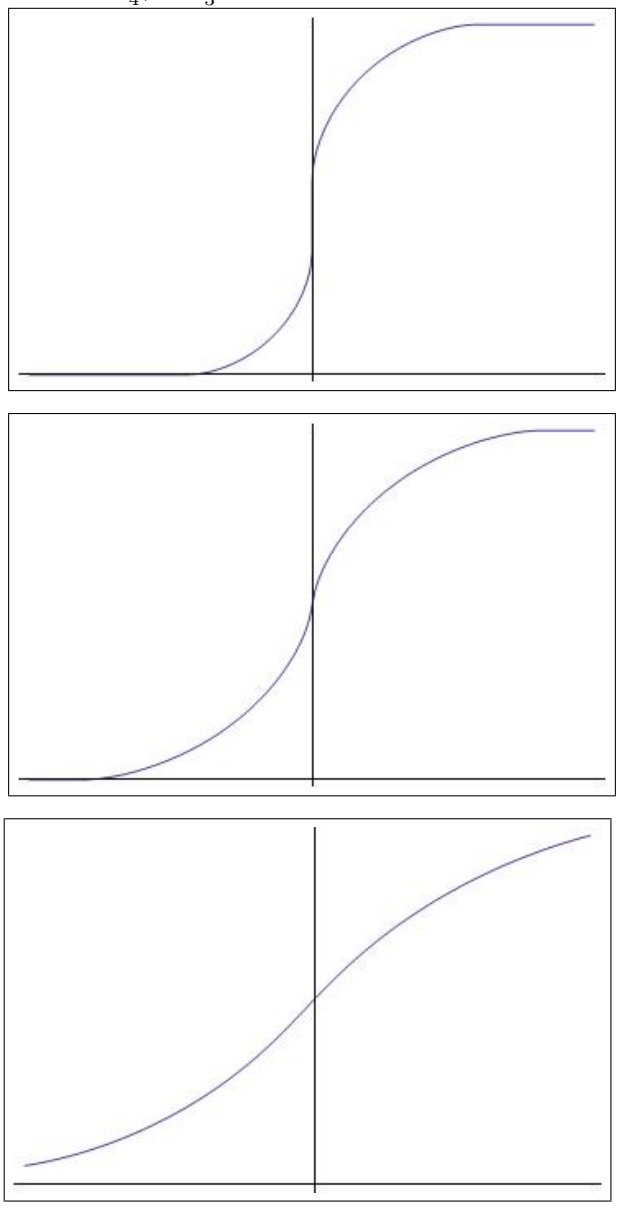

in the u-contour if $s < t$. This kernel for $s = t$ is equivalent to the discrete Bessel kernel $\mathbb{K}_{\text{Bessel}}$, which appears when analyzing Plancherel measures for symmetric groups (see e.g., §2.4 of [20]). Additionally, $\mathbb{J}$ is a special case of the kernel ([11], (3.3)) corresponding to $\theta(t) = e^{-2t}$.

Theorem 4.1. *Let $x_1, \dots, x_k$ be finite and constant. Let $n_1, \dots, n_k$ and $\gamma^{\pm}$ depend on N in such a way that $n_j/N \to t_j$ and $\gamma^{\pm} N \to a > 0$. Then as $N \to \infty$,*

$$\det[K(n_i, x_i; n_j, x_j)]_{1 \le i,j \le k} \to \det[\mathbb{J}(at_i, x_i; at_j, x_j)]_{1 \le i,j \le k}$$

Proof. We use the integral representation for the kernel in Theorem 3.2.

We first focus our attention on the double integral in u and w. Since the integrand is holomorphic everywhere except at $u = 0$, $w = 1$, $w = u$ and $w = 0$, we can deform the contours of integration as shown in Figure 5.

Figure 5: Deformation of the contours.

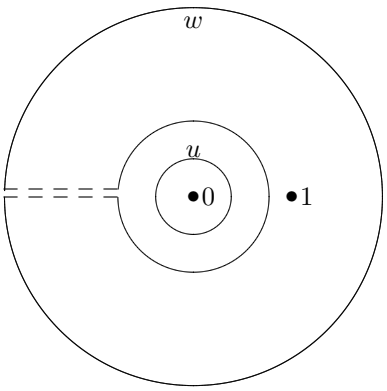

As $N \to \infty$, the integrand converges to 0 for $|w|$ large enough because $|1 - w| \gg |1 - u|$. Therefore we can ignore the outer half of the w contour. Then the contours of integration can be deformed to $|u| = a/N$ and $|w| = 2a/N$. Making the substitutions $u' = Nu/a$ and $w' = Nw/a$, the double integral is now

$$\frac{1}{(2\pi i)^2} \oint_{|u'|=1} \oint_{|w'|=2} \frac{e^{\gamma^+ u'^{-1} N/a + \gamma^- u' a/N}}{e^{\gamma^+ w'^{-1} N/a + \gamma^- w' a/N}} \frac{u'^{x_i} (1 - u'a/N)^{n_i}}{w'^{x_j+1} (1 - w'a/N)^{n_j}} \frac{du' dw'}{w' - u'} \left(\frac{N}{a}\right)^{x_j - x_i}$$

$$= \frac{1}{(2\pi i)^2} \oint_{|u'|=1} \oint_{|w'|=2} \frac{e^{u'^{-1} - at_i u' - w'^{-1} + at_j w' + O(1/N)}}{w' - u'} \frac{dudw}{u'^{-x_i} w'^{x_j+1}} (N/a)^{x_j - x_i}$$

When taking the determinant, the term $(N/\sqrt{a})^{x_j-x_i}$ cancels. This gives the result.

Remark. Comparing this result to [8], we see that the distribution of λ^+ converges to the Poissonized Plancherel measure for the symmetric groups. By the symmetry $(\lambda^\pm \leftrightarrow \lambda^\mp, \gamma^\pm \leftrightarrow \gamma^\mp)$ the same is true for λ^-. On the other hand, a similar contour integral argument to the above shows that $K(n_i, x_i; n_j, -n_j - x_j - 1) \to 0$ as $N \to \infty$, which implies that λ^+ and λ^- are asymptotically independent. □

4.3 Bulk Limits with $\gamma^\pm$ fixed

To state the next result, we need a definition. Given a complex number z_+ in the upper half plane, define

$$S_{z_+}(t_i - t_j; x_i - x_j) = \frac{1}{2\pi i} \int_{\overline{z_+}}^{z_+} u^{x_i - x_j - 1} e^{(t_j - t_i)u} du.$$

If $t_i \geq t_j$, then the integration contour crosses $(0, \infty)$ but does not cross $(-\infty, 0)$. If $t_i < t_j$, then the integration contour crosses $(-\infty, 0)$ but not $(0, \infty)$. This kernel is one of the extensions of the discrete sine kernel constricted to [5]. A similar kernel appeared in [11]. It can be seen as a degeneration of the incomplete beta kernel, see Section 4.4.

The main theorem of this section is the following:

Theorem 4.2. *Let $x_1, \dots, x_k$ and $n_1, \dots, n_k$ all depend on N in such a way that $x_i - x_j$ is constant, $(n_j - N)/\sqrt{N} \to t_j \in \mathbb{R}$ and $x_i/\sqrt{N} \to c \in \mathbb{R}$ for all $1 \leq i, j \leq k$. Write z_+ for $(c + \sqrt{c^2 - 4\gamma^+})/2$. Then*

$$\lim_{N \to \infty} \det[K(n_i, x_i; n_j, x_j)]_{1 \leq i,j \leq k} =$$

$$\begin{cases} 0, & c \geq 2\sqrt{\gamma^+}, \\ 1, & c \leq -2\sqrt{\gamma^+}, \\ \det[S_{z_+}(t_i - t_j; x_i - x_j)]_{1 \leq i,j \leq k}, & -2\sqrt{\gamma^+} < c < 2\sqrt{\gamma^+}. \end{cases}$$

Remark. Theorem 4.2 only makes a statement about the behavior around the top limit curve in Figure 3. If we replace x_i with $-x_i - n_i - 1$ and γ^+ with γ^-, then by symmetry the same statement holds for the asymptotics around the lower Young diagram.

Corollary 4.3. *Let $\rho_1(N, x)$ be the density function of $\mathcal{P}_N^{\gamma^+, \gamma^-}$. Then $\lim_{N \to \infty} \rho_1(N, \alpha N + \beta N^{1/2})$ equals*

- *0, if $\alpha > 0$ or $\alpha < -1$ or $\alpha = 0, \beta \geq 2\sqrt{\gamma^+}$ or $\alpha = -1, \beta \leq -2\sqrt{\gamma^+}$.*
- *1 if $-1 \leq \alpha < 0$ or $\alpha = 0, \beta < -2\sqrt{\gamma^+}$ or $\alpha = -1, \beta \geq 2\sqrt{\gamma^+}$.*
- *$\frac{1}{\pi} \arccos\left(\frac{\beta}{2\sqrt{\gamma^+}}\right)$ if $\alpha = 0, -2\sqrt{\gamma^+} < \beta < 2\sqrt{\gamma^+}$ or $\alpha = -1, -2\sqrt{\gamma^+} < \beta < 2\sqrt{\gamma^+}$.*

Proof. The arguments are similar to those used for the analysis of Plancherel measures for the symmetric groups in [20].

For reasons that will later become clear, it is more convenient to analyze $\sqrt{N}^{x_i-x_j}\sqrt{\gamma^+}^{x_j-x_i}K(n_i,x_i;n_j,x_j)$. When taking the determinant

$$\det[\sqrt{N}^{x_i-x_j}\sqrt{\gamma^+}^{x_j-x_i}K(n_i,x_i;n_j,x_j)],$$

the term $\sqrt{N}^{x_i-x_j}\sqrt{\gamma^+}^{x_j-x_i}$ cancels out.

We use the integral representation for the kernel in Theorem 3.2. The conditions $n_i \geq n_j$ and $n_i < n_j$ translate to $t_i \geq t_j$ and $t_i < t_j$, respectively.

Just as in Theorem 4.1, we can deform the contours of integration as shown in Figure 5.

As $N \to \infty$, the integrand converges to 0 for $|w|$ large enough because $|1-w| \gg |1-u|$. Therefore we can ignore the outer half of the w contour. Then the contours of integration can be deformed to $|u| = 1/\sqrt{N}$ and $|w| = 2/\sqrt{N}$. Making the substitutions $u' = \sqrt{N}u$ and $w' = \sqrt{N}w$, the double integral is now

$$\begin{aligned}
&\frac{1}{(2\pi i)^2}\oint_{|u|=1/\sqrt{N}}\oint_{|w|=2/\sqrt{N}}\frac{e^{\gamma^+u^{-1}+\gamma^-u}}{e^{\gamma^+w^{-1}+\gamma^-w}}\frac{u^{x_i}e^{n_i\ln(1-u)}}{w^{x_j+1}e^{n_j\ln(1-w)}}\frac{dudw}{w-u}\sqrt{N}^{x_i-x_j}\sqrt{\gamma^+}^{x_j-x_i}\\
=&\frac{1}{(2\pi i)^2}\oint_{|u'|=1}\oint_{|w'|=2}\frac{e^{\gamma^+u'^{-1}\sqrt{N}+\gamma^-u'/\sqrt{N}}}{e^{\gamma^+w'^{-1}\sqrt{N}+\gamma^-w'/\sqrt{N}}}\frac{u'^{x_i}e^{n_i\ln(1-u'/\sqrt{N})}}{w'^{x_j+1}e^{n_j\ln(1-w'/\sqrt{N})}}\frac{du'dw'}{w'-u'}\sqrt{\gamma^+}^{x_j-x_i}\\
=&\frac{1}{(2\pi i)^2}\oint_{|u'|=1}\oint_{|w'|=2}\frac{e^{\sqrt{N}(\gamma^+u'^{-1}+c\log u'-u'+O(1/\sqrt{N}))}}{e^{\sqrt{N}(\gamma^+w'^{-1}+c\log w'-w'+O(1/\sqrt{N}))}}\frac{du'dw'}{w'(w'-u')}\sqrt{\gamma^+}^{x_j-x_i}
\end{aligned}$$

In general $|e^z| = e^{\Re z}$, so consider the real part of the function in the exponent, $A(z) = \gamma^+z^{-1} + c\log z - z$. Note that $A'(z) = 0$ at $z_\pm = \frac{c}{2} \pm \frac{\sqrt{c^2-4\gamma^+}}{2}$.

The basic idea of the rest of the proof can be summarized as follows. The term $\sqrt{\gamma^+}^{x_j-x_i}$ creates a $e^{\sqrt{N}(-c\log\sqrt{\gamma^+})}$ term in both the numerator and denominator. So it is equivalent to analyze $\Re(A(z) - c\log\sqrt{\gamma^+}) = \Re(A(z) - A(z_+))$. We deform the u and w contours in such a way that $\Re(A(u)-A(z_+)) < 0$ and $\Re(A(w) - A(z_+)) > 0$, which will cause the integrand to converge to 0 as $N \to 0$. However, the deformation of the contours causes the integral to pick up residues at $u = w$. These residues occur on a circular arc from z_- to z_+. If $c = 2\sqrt{\gamma^+}$, then $z_+ = z_- > 0$, so the arc consists of a single point. As c decreases, z_+ moves counterclockwise around the circle $|z| = \sqrt{\gamma^+}$ while z_- moves clockwise. This means that the arc becomes increasingly large as c decreases from $2\sqrt{\gamma^+}$ to $-2\sqrt{\gamma^+}$. When $c = -2\sqrt{\gamma^+}$, then $z_+ = z_- < 0$, so the arc has becomes the whole circle around the origin.

We then need to consider

$$-\frac{1}{2\pi i}\oint_{|z|=r<1}\frac{z^{x_i-x_j-1}}{(1-z)^{n_j-n_i}}dz,$$

which occurs when $n_i < n_j$. The expression for the residue at $u = w$ has the same integrand. With the minus sign, the integration contour for z goes clockwise along a circle around the origin. Therefore it will cancel the circular arc from z_- to z_+. This explains why the integration contour in S_{z_+} crosses $(0, \infty)$ when $t_i \geq t_j$ and $(-\infty, 0)$ when $t_i < t_j$.

Case 1: $-2\sqrt{\gamma^+} < c < 2\sqrt{\gamma^+}$. Observe that $\Re(A(z) - A(z_+)) = 0$ for all $|z| = |z_\pm| = |\sqrt{\gamma^+}|$. Also notice that $A(z) - A(z_+)$ has a double zero at z_+ and z_-. See Figure 6.

Figure 6: On the left is $\Re(A(z) - c \log \sqrt{\gamma^+})$, where the black regions indicate $\Re < 0$ and the white regions indicate $\Re > 0$.

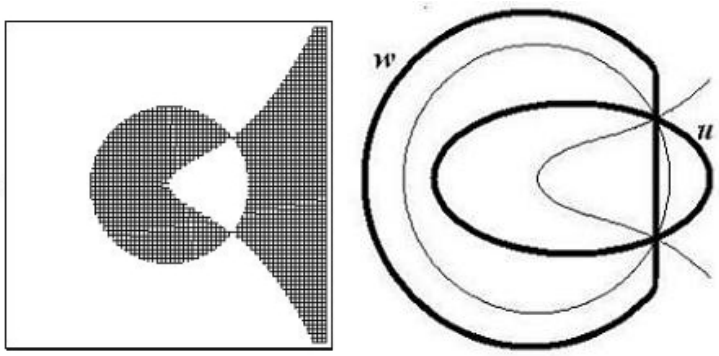

If the contours of integration are deformed as shown in Figure 6, then

$$\frac{e^{\sqrt{N}(\gamma^+ u'^{-1} + c \log u' - u' + O(1/\sqrt{N}))}}{e^{\sqrt{N}(\gamma^+ w'^{-1} + c \log w' - w' + O(1/\sqrt{N}))}} \to 0$$

as $N \to \infty$. The integral thus approaches zero, except for the residues at $u = w$. So $\sqrt{N}^{x_i - x_j} K(n_i, x_i; n_j, x_j)$ converges to

$$\sqrt{N}^{x_i - x_j} \frac{1}{2\pi i} \int_{z_-/\sqrt{N}}^{z_+/\sqrt{N}} \frac{du}{u^{x_j - x_i + 1}} (1-u)^{n_i - n_j} \to \frac{1}{2\pi i} \int_{z_-}^{z_+} u^{x_i - x_j - 1} e^{-(t_i - t_j)u} du$$

.

If $t_i \geq t_j$, then the integration contour crosses $(0, \infty)$. If $t_i < t_j$, then the contour crosses $(-\infty, 0)$.

Case 2: $c^2 - 4\gamma^+ > 0$ and $c > 0$. Deforming the contours of integration as shown in Figure 7, the integral becomes zero. The contours do not pass through each other, so no residues appear. So $\sqrt{N}^{x_i - x_j} K(n_i, x_i; n_j, x_j) \to 0$ if $t_i \geq t_j$. This means that $\det[K(n_i, x_i; n_j, x_j)] \to 0$.

Case 3: $c^2 - 4\gamma^+ > 0$ and $c < 0$. Deform the contours as shown in Figure 8. Since the w and u contours pass through each other during the deformation, the integral picks up residues at $u = w$. So if $t_i \geq t_j$, then $\sqrt{N}^{x_i - x_j} K(n_i, x_i; n_j, x_j)$ converges to

Figure 7: Again, the figure on the left shows $\Re(A(z)-A(z_+))$, with black regions indicating $\Re < 0$ and white regions indicating $\Re > 0$.

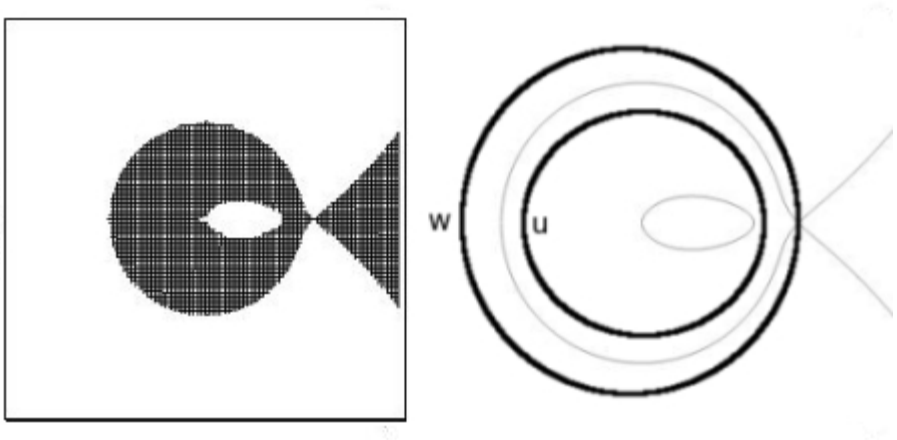

$$\sqrt{N}^{x_i-x_j}\frac{1}{2\pi i}\oint w^{x_i-x_j-1}(1-w)^{n_i-n_j}dw = \frac{1}{2\pi i}\oint w^{x_i-x_j-1}e^{(t_j-t_i)w}dw$$
$$= \frac{(t_j-t_i)^{x_j-x_i}}{(x_j-x_i)!}$$

If $t_i < t_j$, then there is the integral in z, which cancels with the residues at $u = w$, so $\sqrt{N}^{x_i-x_j}K(n_i, x_i; n_j, x_j)$ converges to 0. This means that the matrix $[K(n_i, x_i; n_j, x_j)]$ asymptotically has ones on the diagonal and zeroes below. So $\det[K(n_i, x_i; n_j, x_j)]$ converges to 1.

□

Remark. It is natural to ask what happens when $x_i/\sqrt{n_i}$ do not all converge to the same real number. When this occurs, the determinant $\det[K(n_i, x_i; n_j, x_j)]$ factors into blocks corresponding to distinct values of $\lim x_i/\sqrt{n_i}$. Probabilistically, this means that the probability of finding a vertical edge becomes independent in different parts of the boundary.

4.4 Bulk Limits with $\gamma^{\pm} \propto N$

We now let $\gamma^{\pm}$ depend on N in such a way that $\gamma^+/N \to a > 0$ and $\gamma^-/N \to b > 0$ as $N \to \infty$. Before we can state the result, some preliminary definitions and lemmas are needed.

For $a, b > 0$ and $c \in \mathbb{R}$, recall that

$$R_{a,b,c}(z) = -bz^3 + (b-c-1)z^2 + (c+a)z - a.$$

Figure 8: On the left is $\Re(A(z) - c\log\sqrt{\gamma^+})$, where the black regions indicate $\Re < 0$ and the white regions indicate $\Re > 0$.

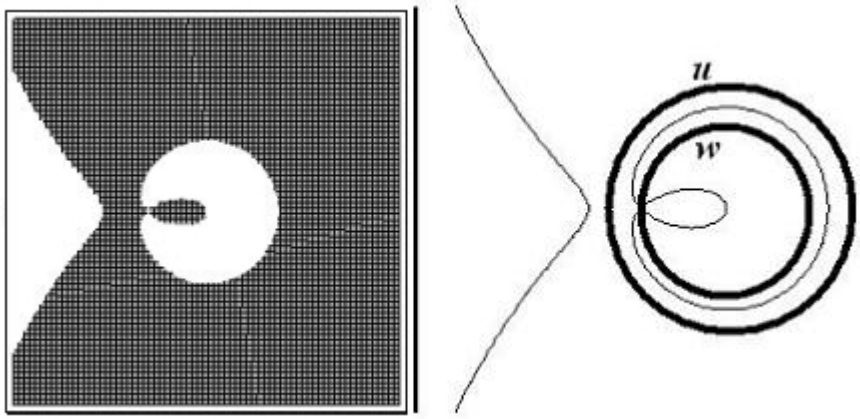

Lemma 4.4. *(1) The cubic polynomial $R_{a,b,c}(z)$ has a multiple root iff c is a root of $Q_{a,b}(z)$, where $Q_{a,b}(z)$ is defined in §3.1.*

(2) Let $q_1 \le \ldots \le q_m$ be the real roots of $Q_{a,b}$. If $q_1 < c < q_2$ or $q_{m-1} < c < q_m$ then $R_{a,b,c}(z)$ has a pair of complex conjugate roots.

Proof. (1) In general, a polynomial has a multiple root iff its discriminant is zero. The discriminant of $R_{a,b,c}$ is exactly $Q_{a,b}(c)/16$.

(2) A cubic polynomial has nonreal roots iff its discriminant is negative. Since $Q_{a,b}$ diverges to $+\infty$ in both directions, $Q_{a,b}(z)$ is negative for $q_1 < z < q_2$ and $q_{m-1} < z < q_m$. □

Lemma 4.5. *The polynomial $Q_{a,b}$ has a double root at c_0 iff a, b and c_0 satisfy the equations*

$$a = \frac{z_0^3}{(z_0-1)^3}, \quad b = -\frac{1}{(z_0-1)^3}, \quad c_0 = -\frac{z_0^2(z_0-3)}{(z_0-1)^3} \tag{9}$$

for some $z_0 \in \mathbb{R}$.

Proof. Since $Q_{a,b}(c_0)$ is the discriminant of R_{a,b,c_0}, $Q_{a,b}(z)$ has a double root at c_0 iff $R_{a,b,c_0}(z)$ has a triple root. For any z_0, R has a triple root at z_0 iff $R(z_0) = R'(z_0) = R''(z_0) = 0$. This gives three linear equations in the three variables a, b, and c_0, which can be solved explicitly. □

Remark. We have $a, b > 0$ iff $z_0 < 0$. Then $-1 < c_0 < 0$.

One more definition is needed before we can state the main result of this section. Let B be the incomplete beta kernel defined by

$$\mathrm{B}_z(k,l) = \frac{1}{2\pi i}\int_{\bar{z}}^{z} (1-u)^k u^{-l-1} du,$$

Figure 9: This figure shows the equations in (9), with a plotted on the horizontal axis and b plotted on the vertical with parameter z_0.

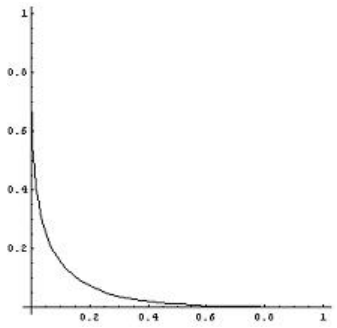

where the path of integration crosses $(0,1)$ for $k \geq 0$ and $(-\infty, 0)$ for $k < 0$. The incomplete beta kernel has been introduced in [23]. It is one of the extensions of the discrete sine kernel of [5].

Theorem 4.6. *Let $\gamma^+/N \to a$ and $\gamma^-/N \to b$ for positive real numbers a and b. Also let $x_1, \ldots, x_k$ and $n_1, \ldots, n_k$ depend on N in such a way that $n_i - n_j$ and are $x_i - x_j$ constant, $n_j/N \to 1$ and $x_j/N \to c$ for all $1 \leq i, j \leq k$. Let $q_1 \leq \ldots \leq q_m$ denote the distinct real roots of $Q_{a,b}(x)$ (m can be 2,3, or 4). Additionally, assume $Q_{a,b}(c) \neq 0$. Let z_+ be a root of $R_{a,b,c}(x)$ such that $\Im(z_+) \geq 0$ (cf. Lemma 4.4). If $m = 4$, then*

$$\det[K(n_i, x_i; n_j, x_j)]_{1 \leq i,j \leq k} \to \begin{cases} 0, & c \leq q_1, \\ \det[\mathrm{B}(n_i - n_j, x_j - x_i; z_+)]_{1 \leq i,j \leq k}, & q_1 < c < q_2, \\ 1, & q_2 \leq c \leq q_3, \\ \det[\mathrm{B}(n_i - n_j, x_j - x_i; z_+)]_{1 \leq i,j \leq k}, & q_3 < c < q_4, \\ 0, & c \geq q_4. \end{cases}$$

If $m = 2$ or 3, then

$$\det[K(n_i, x_i; n_j, x_j)]_{1 \leq i,j \leq k} \to \begin{cases} 0, & c \leq q_1, \\ \det[\mathrm{B}(n_i - n_j, x_j - x_i; z_+)]_{1 \leq i,j \leq k}, & q_1 < c < q_m, \\ 0, & c \geq q_m, \end{cases}$$

Proof. The double integral in the correlation kernel of Theorem 3.2 asymptotically becomes

$$\left(\frac{1}{2\pi i}\right)^2 \oint \oint \frac{e^{N(au^{-1} + bu + c\log(u) + \log(1-u) + O(1/N))}}{e^{N(aw^{-1} + bw + c\log(u) + \log(1-u) + O(1/N))}} \frac{dudw}{w(u-w)}$$

where the contours are over $|u| = r$ and $|w - 1| = \epsilon < 1 - r$. So we can perform a similar analysis as in Theorem 4.2, except with a more complicated

Figure 10: The shaded regions show $\Re(A(z;c) - A(z_+;c)) < 0$, while the white regions show $\Re > 0$. The first row corresponds to $c < q_1$, the second row corresponds to $q_1 < c < q_2$, the third corresponds to $q_2 < c < q_3$, the fourth corresponds to $q_3 < c < q_4$, and the fifth corresponds to $c > q_4$.

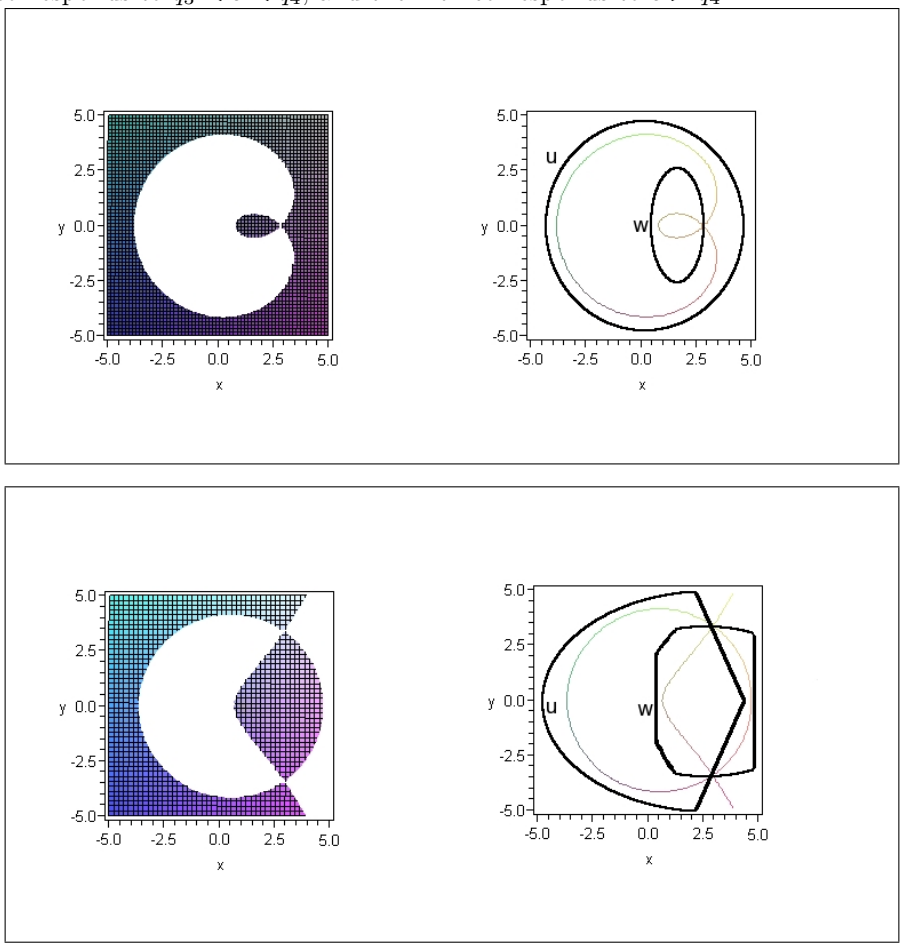

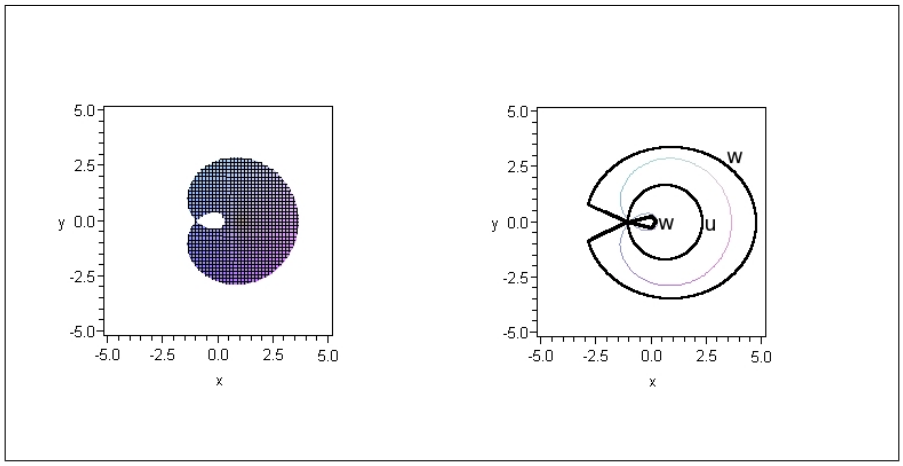
5.0
2.5
y 0.0
-2.5
-5.0
-5.0 -2.5 0.0 2.5 5.0
x
w
w
u

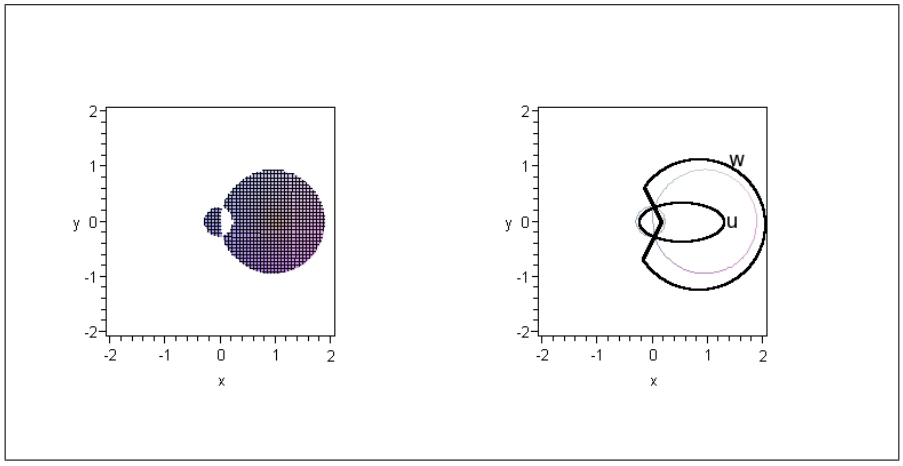
2
1
y 0
-1
-2
-2 -1 0 1 2
x
w
u

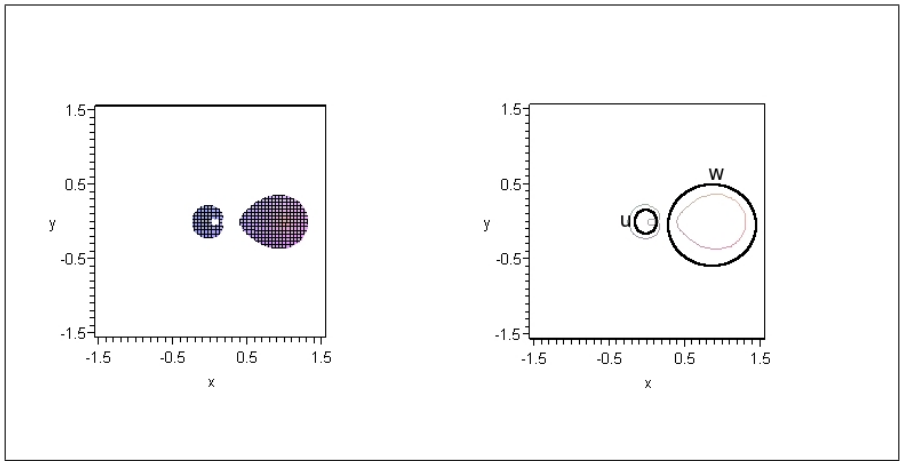
1.5
0.5
y
-0.5
-1.5
-1.5 -0.5 0.5 1.5
x
w
u

$A(z) = az^{-1} + bz + c\log(z) + \log(1-z)$. For this proof, it is actually more convenient to write $A(z;c)$ in place of $A(z)$.

First we find which values of c correspond to the edges of the hypothetical limit shape in Figure 4. These are the values of c such that $A(z;c) - A(z_0;c)$ has a triple zero for some $z_0 \in \mathbb{C}$. Requiring $A(z;c) - A(z_0;c)$ to have a triple zero at $z = z_0$ is equivalent to requiring $A'(z;c)$ to have a double zero at $z = z_0$. Multiplying the equation $A'(z;c) = 0$ by $z^2(1-z)$ gives the equation $R_{a,b,c}(z) = 0$ (Note that $R_{a,b,c}(0) = -a$ and $R_{a,b,c}(1) = -1$, which are both nonzero). By Lemma 4.4, $R_{a,b,c}$ has a double zero iff $c = q_1, \ldots, q_m$.

Now we need to determine how to appropriately deform the contours. The analysis here is almost identical to that of Thereom 4.2. We want to find nonreal values of z_0 such that $A(z;c) - A(z_0;c)$ has a double zero. This reduces to looking for nonreal roots of $R_{a,b,c}(z)$ in the upper half-plane, which we have defined to be z_+. As can be seen from Figure 4, there are potentially five different regions of behavior for the bulk limits. The corresponding behavior of $\Re(A(z;c) - A(z_+;c))$ is shown in Figure 10. (These are computer generated figures for specific values of parameters, however, it is not hard to prove that similar figures arise for any values of the parameters in the corresponding domains. An example of such an argument can be found in the beginning of the proof of Theorem 4.7 below.) The arguments of Theorem 4.2 are again applicable here, except with the new definition of z_+. □

4.5 The Pearcey Kernel as an Edge Limit

We now find the edge limit at the point where the two limit curves in the middle figure in Figure 4 just barely merge. In this case, we analyze the limiting behavior of K_Δ from Corollary 3.3 instead of K, which corresponds to the fact that we consider the limit of the point process formed by columns of $\lambda^{\pm}$ rather than by their rows, see Figure 1.

Theorem 4.7. *Fix $z_0 < 0$ and let a, b and c_0 satisfy equations (9). Let $\gamma^+/N \to a$ and $\gamma^-/N \to b$ as $N \to \infty$. Let $n_1, \ldots, n_k$ depend on N in such a way that $(n_j - N)/\sqrt{N} \to 2t_j \in \mathbb{R}$ as $N \to \infty$. Set $\zeta = (z_0 - 1)|z_0|^{-1/2} < 0$. Define*

$$\tilde{t}_j = \frac{z_0}{1 - z_0} t_j$$

and let $x_1, \ldots, x_k$ depend on N in such a way that

$$\frac{\zeta(x_j - c_0 N - \tilde{t}_j\sqrt{N})}{N^{1/4}} \to s_j \in \mathbb{R}$$

as $N \to \infty$. Then as $N \to \infty$,

$$\det[-\zeta^{-1} N^{1/4} K_\Delta(n_i, x_i; n_j, x_j)]_{1 \le i,j \le k} \to \det[P(t_i, s_i; t_j, s_j)]_{1 \le i,j \le k}$$

where

$$
\begin{aligned}
&P(t_i, s_i; t_j, s_j) \\
&= \left(\frac{1}{2\pi i}\right)^2 \int\int e^{w^4-u^4+t_i u^2-t_j w^2+s_i u-s_j w} \frac{du dw}{u-w} \\
&\qquad -\frac{1}{\sqrt{2\pi|t_i-t_j|}} \exp\left(-\frac{(s_j-s_i)^2}{2(t_i-t_j)}\right), \qquad t_i > t_j \\
&\left(\frac{1}{2\pi i}\right)^2 \int\int e^{w^4-u^4+t_i u^2-t_j w^2+s_i u-s_j w} \frac{du dw}{u-w}, \qquad t_i \le t_j
\end{aligned} \tag{10}
$$

where u is integrated from $-i\infty$ to $i\infty$ and w is integrated on the rays from $\pm\infty e^{i\pi/4}$ to 0 and from $\pm\infty e^{-i\pi/4}$ to 0 as in Figures 11 and 12.

Figure 11: The contour for u.

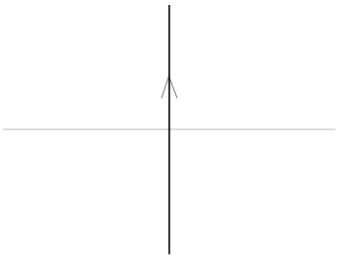

Figure 12: The contour for w.

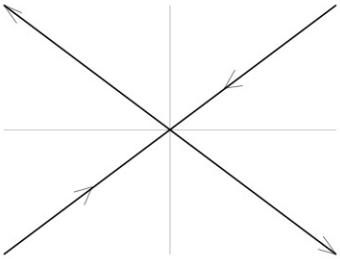

The kernel $P(t_i, s_i; t_j, s_j)$ is called the Pearcey kernel and it was previously obtained in [1],[13],[14],[24],[27].

Proof. The argument is similar to the proofs of Theorems 4.2 and 4.6. It is convenient to let $A(z; c; d)$ denote $az^{-1} + bz + c\log z + d\log(1-z)$. Then the

double integral in the correlation kernel of Corollary 3.3 becomes asymptotically

$$-\left(\frac{1}{2\pi i}\right)^2 \int\int \frac{e^{N(au^{-1}+bu+(x_i/N)\log u+(n_i/N)\log(1-u)+O(1/N))}}{e^{N(aw^{-1}+bw+(x_j/N)\log w+(n_j/N)\log(1-w)+O(1/N))}} \frac{dudw}{w(u-w)} \tag{11}$$

$$= -\left(\frac{1}{2\pi i}\right)^2 \int\int \frac{e^{N(A(u;x_i/N;n_i/N)+O(1/N))}}{e^{N(A(w;x_j/N;n_j/N)+O(1/N))}} \frac{dudw}{w(u-w)} \tag{12}$$

Multiplying the integrand by the conjugating factor

$$\frac{e^{-NA(z_0;x_i/N;n_i/N)}}{e^{-NA(z_0;x_j/N;n_j/N)}} = \frac{z_0^{-x_i}}{z_0^{-x_j}} \frac{(1-z_0)^{-n_i}}{(1-z_0)^{-n_j}} \frac{e^{-aNz_0^{-1}}}{e^{-aNz_0^{-1}}} \frac{e^{-bNz_0}}{e^{-bNz_0}},$$

which cancels when taking the determinant for correlation functions, allows us to consider $A(z;x_m/N;n_m/N)-A(z_0;x_m/N;n_m/N)$ instead of $A(z;x_m/N;n_m/N)$.

Figure 13: The figure on the left shows $\Re(A(z;c_0;1)-A(z_0;c_0;1))$, with black regions indiciating $\Re<0$ and white regions indicating $\Re>0$.

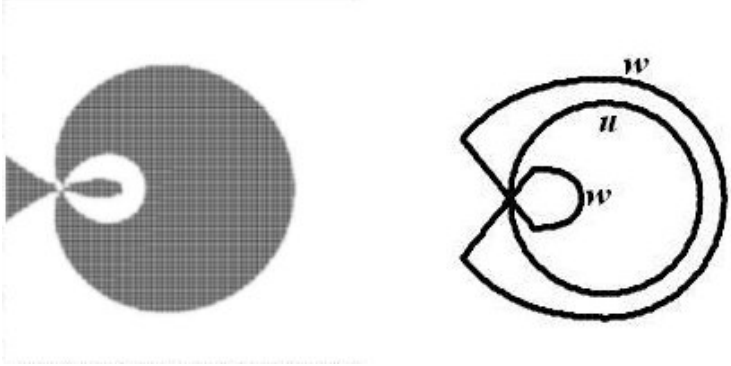

Deform the contours as shown in Figure 13. Let us show that these contours exist. We know that the level lines only intersect at z_0 (the only critical point of the function $A(z;c_0;1)-A(z_0;c_0;1)$, since $A'(z)=-b(z-z_0)^3z^{-2}(1-z)^{-1}$), and they are symmetric with respect to the real axis. Restrict $\Re(A(z;c_0;1)-A(z_0;c_0;1))$ to the real axis. For $|x|=\epsilon$ small, the main contribution to $\Re(A(x;c_0;1))$ comes from the term ax^{-1}. So $\Re(A(x;c_0;1))$ is positive at $x=\epsilon>0$ and negative at $x=\epsilon<0$, so the level lines cross the real axis at 0. For $x=1-\epsilon$ with ϵ small, the main contribution to $\Re(A)$ comes from the term $\log|1-x|$. This implies that $\Re(A)$ is negative $x=1-\epsilon$, so the level lines cross the real axis somewhere between 0 and 1. For large x, the main contribution to $\Re(A)$ comes from bx, so $\Re(A)$ is positive for large x. Therefore the level lines cross the real axis at a third point. Since $A'(z)=-b(z-z_0)^3z^{-2}(1-z)^{-1}$ is positive for $z<z_0$, negative for $z\in(z_0,0)\cup(0,1)$, and positive for $z>1$, the levels lines can not intersect the real axis at any other point.

For a fixed $x \ll 0$, the main contribution to $\Re(A(x))$ comes from bx, so $\Re(A(x))$ is negative. However, as y increases, $\Re(A(x+iy))$ goes to $+\infty$, since the main contributions come from $c_0 \log|x+iy| + \log|1-x-iy|$, and $c_0 > -1$. This means there must be level lines going off to infinity. Restricting $\Re(A(z; c_0; 1))$ to a circle $|z| = R \gg 1$ shows that these are the only level lines that go to infinity. Indeed, note that $\Re(A(z; c_0; 1)) > 0$ if $z = R$, and as z moves counterclockwise around the circle, the main contribution to the changes in $\Re(A(z))$ comes from bz. Thus $\Re(A(z))$ decreases as z moves counterclockwise around the circle in the upper half-plane, so the circle can intersect at most one level line in the upper half-plane.

In the upper half-plane, there are four level lines coming from the critical point z_0. We know that three of these lines cross the real axis, while one of them goes off to infinity. Since they can only intersect at z_0, the only possibility is a picture as shown in Figure 13. This justifies the existence of the contours.

These deformations cause the kernel to pick up residues at $u = w$. The expression for these residues is

$$-\frac{1}{2\pi i} \oint \frac{z^{x_i - x_j - 1}}{(1-z)^{n_j - n_i}} dz \tag{13}$$

where the integral goes around a circle $|z| < 1$. If $n_i \leq n_j$, then expression (13) cancels with the z-contour in expression (5). If $n_i > n_j$, then explicitly evaluating the integral yields

$$-(-1)^{x_j - x_i} \binom{n_i - n_j}{x_j - x_i}.$$

The binomial can be approximated by the deMoivre-Laplace Theorem. For large N,

$$\begin{aligned} &-N^{1/4} z_0^{x_j - x_i} (1-z_0)^{n_j - n_i} (-1)^{x_j - x_i} \binom{n_i - n_j}{x_j - x_i} \\ &\approx -\frac{1}{\sqrt{2\pi(t_i - t_j)}} \exp\left(-\frac{(s_j - s_i)^2}{2(t_i - t_j)} \right). \end{aligned}$$

So when $t_i > t_j$, we obtain the extra exponential term in equation (10).

For large values of N, all the contributions to the double integral come from near the point z_0. Taking the Taylor expansion around z_0 yields

$$\begin{aligned} &N\left(A\left(z; c_0 + \frac{\tilde{t}_m}{N^{1/2}} + \frac{u_m}{N^{3/4}}; 1 + \frac{2t_m}{N^{1/2}} \right) - A\left(z_0; c_0 + \frac{\tilde{t}_m}{N^{1/2}} + \frac{u_m}{N^{3/4}}; 1 + \frac{2t_m}{N^{1/2}} \right) \right) \\ &= s_m z' + t_m (z')^2 - (z')^4 + o(1) \end{aligned}$$

where $z' = z_0^{-1} \zeta^{-1} N^{1/4} (z - z_0)$. This suggests the substitutions

$$u' = z_0^{-1} \zeta^{-1} N^{1/4} (u - z_0), \quad w' = z_0^{-1} \zeta^{-1} N^{1/4} (w - z_0).$$

By making these substitutions, we are zooming in at the point z_0 in Figure 13. Then u' is integrated as shown in Figure 11 while w' is integrated as shown in Figure 12.

The exponential terms in expression (12) converge to the exponential terms in (10). The term $\frac{dudw}{u-w}$ turns into $z_0\zeta N^{-1/4}\frac{du'dw'}{u'-w'}$. For large N, the contributions to the correlation kernel become focused around z_0, so the extra w in the denominator becomes z_0^{-1}. The proof of Theorem 4.7 is complete. □

4.6 The Airy Kernel as an Edge Limit

Before stating the main result, some definitions are needed.

Let $Ai(x)$ denote the Airy function:

$$Ai(x) = \frac{1}{2\pi}\int_{-\infty}^{\infty} e^{is^3/3+ixs}ds.$$

This integral only converges conditionally. Shift the contour of integration as shown in Figure 14. Along this contour, the function $e^{is^3/3}$ is real and decreases superexponentially.

Figure 14: A better contour for the Airy function. The contour goes from $\infty e^{5\pi i/6}$ to 0 to $e^{\pi i/6}$.

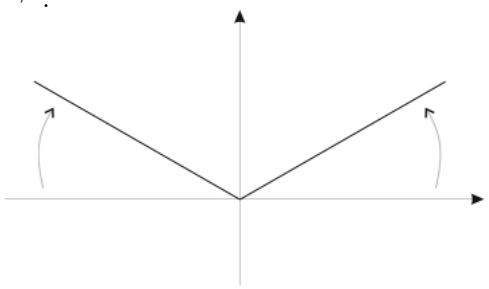

Define the *extended Airy kernel* $\mathcal{A}$ to be

$$\mathcal{A}(\tau_1,\sigma_1;\tau_2,\sigma_2) = \begin{cases} \int_0^{\infty} e^{-\lambda(\tau_1-\tau_2)}Ai(\sigma_1+\lambda)Ai(\sigma_2+\lambda)d\lambda & \text{if } \tau_1 \geq \tau_2, \\ -\int_{-\infty}^{0} e^{-\lambda(\tau_1-\tau_2)}Ai(\sigma_1+\lambda)Ai(\sigma_2+\lambda)d\lambda & \text{if } \tau_1 < \tau_2. \end{cases} \tag{14}$$

It was first obtained in [26] in the context of the polynuclear growth model.

There is a useful representation for $\mathcal{A}$ as a double integral.

Proposition 4.8. *([15], §2.2) Let ν_1, ν_2 satisfy $\nu_1+\nu_2+\tau_1-\tau_2 > 0$. If $\tau_1 \geq \tau_2$, then*

$$\mathcal{A}(\tau_1,\sigma_1;\tau_2,\sigma_2) = \left(\frac{1}{2\pi i}\right)^2 \int_{\Im(u)=\nu_1}\int_{\Im(w)=\nu_2} \frac{e^{i\sigma_1 u+i\sigma_2 w+i(w^3+u^3)/3}}{\tau_2-\tau_1+i(w+u)}dudw.$$

If $\tau_1 < \tau_2$, then

$$\mathcal{A}(\tau_1,\sigma_1;\tau_2,\sigma_2) = \left(\frac{1}{2\pi i}\right)^2 \int_{\Im(u)=\nu_1}\int_{\Im(w)=\nu_2} \frac{e^{i\sigma_1 u + i\sigma_2 w + i(w^3+u^3)/3}}{\tau_2-\tau_1+i(w+u)}dudw$$

$$-\frac{1}{\sqrt{4\pi(\tau_2-\tau_1)}}\exp\left(-\frac{(\sigma_1-\sigma_2)^2}{4(\tau_2-\tau_1)} - \frac{1}{2}(\tau_2-\tau_1)(\sigma_1+\sigma_2) + \frac{1}{12}(\tau_2-\tau_1)^3\right)$$

The double integral from Proposition 4.8 can be rewritten as

$$\left(\frac{1}{2\pi i}\right)^2 \int\int \exp\big(\tau_1\sigma_1 - \tau_2\sigma_2 - \frac{1}{3}\tau_1^3 + \frac{1}{3}\tau_2^3 - (\sigma_1-\tau_1^2)u + (\sigma_2-\tau_2^2)w$$
$$- \tau_1 u^2 + \tau_2 w^2 + \frac{1}{3}(u^3-w^3)\big)\frac{dudw}{u-w}. \quad (15)$$

Indeed, just as we deformed the contours of integration for $Ai(x)$, we can deform the contours of integration in Proposition 4.8. The u-contour can be taken over $i\nu_1 + \infty e^{5\pi i/6}$ to $i\nu_1$ to $i\nu_1 + e^{\pi i/6}$, while the w-contour can be taken from $i\nu_2 + \infty e^{5\pi i/6}$ to $i\nu_2$ to $i\nu_2 + e^{\pi i/6}$. Integrating along these contours also allows for the possibility of $\nu_1+\nu_2+\tau_1-\tau_2 = 0$. If we further make the substitutions $w = -iw' + \nu_2 i$ and $u = iu' + \nu_1 i$, then the double integral becomes

$$\left(\frac{1}{2\pi i}\right)^2 \int\int \exp\big(-\nu_1\sigma_1 - \nu_2\sigma_2 + \frac{1}{3}\nu_1^3 + \frac{1}{3}\nu_2^3 - (\sigma_1-\nu_1^2)u + (\sigma_2-\nu_2^2)w$$
$$+ \nu_1 u^2 + \nu_2 w^2 + \frac{1}{3}(u^3-w^3)\big)\frac{dudw}{-\tau_2+\tau_1+\nu_1+\nu_2+u-w}.$$

where u is integrated from $\infty e^{-\pi i/3}$ to 0 to $\infty e^{\pi i/3}$ and w is integrated from $\infty e^{4\pi i/3}$ to 0 to $\infty e^{2\pi i/3}$. Taking $\nu_1 = -\tau_1$ and $\nu_2 = \tau_2$ turns the double integral into (15). Writing the double integral in this form is useful when proving the following result.

In the next statement, let $Q_{a,b}$ be the same polynomial as in §3.1, see also §3.4.

Theorem 4.9. *Let $\gamma^+/N \to a, \gamma^-/N \to b$ for positive real numbers a and b. Let c_1 be a root of $Q_{a,b}(z)$ and z_1 be the double zero of $R_{a,b,c_1}(z)$. Let $n_1,\ldots,n_k$ depend on N in such a way that*

$$\frac{n_j - N}{N^{2/3}} \to t_j \in \mathbb{R} \text{ as } N\to\infty.$$

Let $\tilde{t}_j = t_j z_1(1-z_1)^{-1}$ and let $x_1,\ldots,x_k$ depend on N in such a way that

$$\frac{x_j - c_1 N - \tilde{t}_j N^{2/3}}{N^{1/3}} \to s_j \in \mathbb{R} \text{ as } N\to\infty.$$

If $c_1 > 0$ or $c_1 < -1$, set $\mathcal{K} = K$. Otherwise, set $\mathcal{K} = K_\Delta$. Then as $N\to\infty$,

$$\det[|z_1 p_3^{1/3}| N^{1/3}\mathcal{K}(n_i,x_i;n_j,x_j)]_{1\le i,j\le k} \to \det[\mathcal{A}(\tau_i,\sigma_i;\tau_j,\sigma_j)]_{1\le i,j\le k}.$$

Here, p_3 denotes the constant

$$-\frac{1}{(1-z_1)^3}-\frac{3a}{z_1^4}+\frac{c_1}{z_1^3}$$

and

$$\tau_m=\frac{t_m}{2(p_3)^{2/3}(z_1-1)^2z_1},\quad \sigma_m=\tau_m^2-\frac{s_m}{z_1p_3^{1/3}},\quad 1\le m\le k.$$

Remark. The statement may seem a bit cryptic. Let us explain it in words. There are (potentially) four edge points as seen in Figure 4. We consider K for the first point (when $c_1>0$) and the fourth point (when $c_1<-1$), which means that we look at the largest rows of λ^+ and λ^-. For the second and third points we consider K_Δ, which means that we look at the largest columns of λ^+ and λ^-. For the second and fourth points, $\det[z_1p_3^{1/3}\mathcal{K}]\to\det[\mathcal{A}]$, while for the first and third points $\det[-z_1p_3^{1/3}\mathcal{K}]\to\det[\mathcal{A}]$. At the second and fourth points $z_1p_3^{1/3}$ is positive, while at the first and third points $z_1p_3^{1/3}$ is negative. This corresponds to the fact that in order to obtain the Airy process we need to flip the sign of particles at the lower edges of λ^+ and λ^- (the second and fourth edge points, respectively).

Proof. This proof is similar to the proof of Theorem 4.7, so some of the details will be omitted.

Once again, let $A(z;c;d)$ denote $az^{-1}+bz+c\log z+d\log(1-z)$. Multiplying by the conjugating factor

$$\frac{e^{-NA(z_1;x_i/N;n_i/N)}}{e^{-NA(z_1;x_j/N;n_j/N)}}=\frac{z_1^{-x_i}}{z_1^{-x_j}}\frac{(1-z_1)^{-n_i}}{(1-z_1)^{-n_j}}\frac{e^{-aNz_1^{-1}}}{e^{-aNz_1^{-1}}}\frac{e^{-bNz_1}}{e^{-bNz_1}}$$

allows us to consider $A(z;x_m/N;n_m/N)-A(z_1;x_m/N;n_m/N)$ instead of $A(z;x_m/N;n_m/N)$. The Taylor expansion yields

$$\begin{aligned}&N\left(A\left(z;c_1+\frac{\tilde{t}_m}{N^{1/3}}+\frac{u_m}{N^{2/3}};1+\frac{t_m}{N^{1/3}}\right)-A\left(z_1;c_1+\frac{\tilde{t}_m}{N^{1/3}}+\frac{u_m}{N^{2/3}};1+\frac{t_m}{N^{1/3}}\right)\right)\\&=\frac{1}{3}(z')^3-\frac{t_m}{2(p_3)^{2/3}(z_1-1)^2z_1}(z')^2+\frac{s_m}{(p_3)^{1/3}z_1}z'+o(1)\end{aligned}$$

where $z'=(p_3)^{1/3}N^{1/3}(z-z_1)$. The contours of integration for u and w are shown in Figure 15. Now let $u'=(p_3)^{1/3}N^{1/3}(u-z_1)$ and $w'=(p_3)^{1/3}N^{1/3}(w-z_1)$. Just like in the proof of Theorem 4.7, the Taylor series gives rise to the exponential terms in 15. In addition, the term $\frac{dudw}{u-w}$ becomes $N^{-1/3}p_3^{-1/3}$, while the extra w in the denominator becomes z_1^{-1}. We break down the following analysis into cases.

Case 1: $c_1>0$. This corresponds to the fourth row in Figure 15 and the top edge point of Figure 3. In this case, p_3 is negative, so the contours for u' and w' agree with the contours in expression (15). Since $0<z_1<1$, this implies that $\tilde{t}_j-\tilde{t}_i>0$ if $t_j-t_i>0$. Since $n_j>n_i$ translates to $t_j>t_i$, this means that

Figure 15: The left column shows $\Re(A(z;c_0;1) - A(z_0;c_0;1))$, with shaded regions showing $\Re < 0$ and white regions showing $\Re > 0$. The right column shows the local behavior around z_1. The first row occurs when c_1 is the smallest real root of $Q_{a,b}$, the second row when c_1 is the second smallest real root, and so forth. If $Q_{a,b}$ has only two real roots, the middle two rows do not occur.

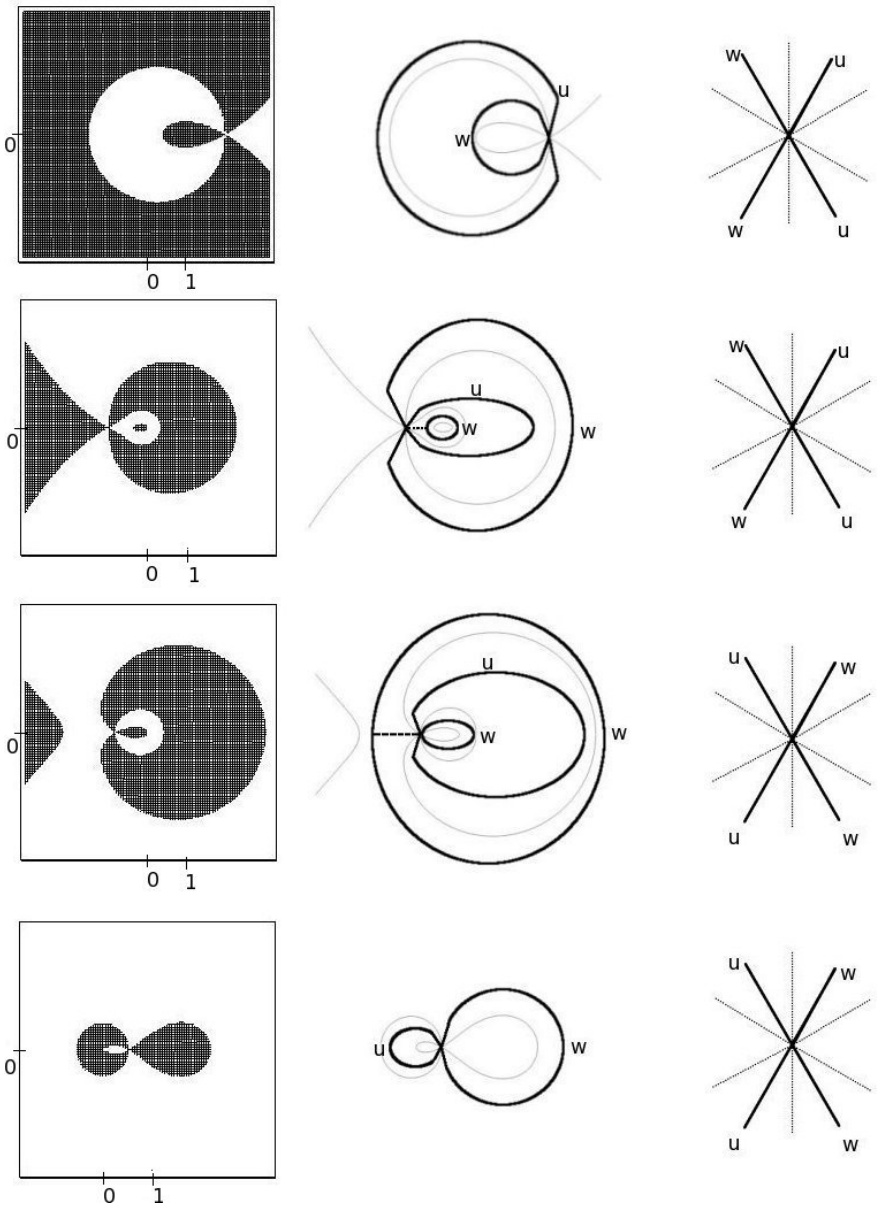

$x_j - x_i$ can be assumed positive if $n_j > n_i$. Therefore the integral in z from expression (4) can be written as

$$-\binom{n_j - n_j + x_j - x_i - 1}{x_j - x_i} = -\binom{n_j - n_i + x_j - x_i}{x_j - x_i} \frac{n_j - n_i}{n_j - n_i + x_j - x_i}.$$

Using the Laplace-Demoivre Theorem shows that

$$-N^{1/3} \frac{z_1^{x_j - x_1}}{(1-z_1)^{n_i - n_j}} \binom{n_j - n_i + x_j - x_i - 1}{x_j - x_i} \to$$

$$-\frac{|1-z_1|}{\sqrt{2\pi |z_1| (t_j - t_i)}} \exp\left(-\frac{(1-z_1)^2}{2|z_1|} \frac{(s_j - s_i)^2}{|t_j - t_i|} \right). \tag{16}$$

Taking the last term in Proposition 4.8 and multiplying by $\exp(-\tau_1\sigma_1 + \tau_2\sigma_2 + \frac{1}{3}\tau_1^3 - \frac{1}{3}\tau_2^3)$ yields

$$-|p_3|^{1/3} |z_1|^{1/2} \frac{|1-z_1|}{\sqrt{2\pi (t_j - t_i)}} \exp\left(-\frac{(1-z_1)^2}{2z_1} \frac{(s_j - s_i)^2}{t_j - t_i} \right).$$

We have seen that

$$|z_1 p_3^{1/3}| N^{1/3} \frac{z_1^{x_j - x_1}}{(1-z_1)^{n_i - n_j}} K(n_i, x_i; n_j, x_j) \to$$
$$\exp(-\tau_1\sigma_1 + \tau_2\sigma_2 + \frac{1}{3}\tau_1^3 - \frac{1}{3}\tau_2^3) \mathcal{A}(\tau_i, \sigma_i; \tau_j, \sigma_j), \tag{17}$$

which gives the result.

Case 2: $c_1 < -1$. This corresponds to the first row in Figure 15. Here, $z_1 > 1$ and $p_3 > 0$. Making the deformations gives residues at $u = w$, which can be written as

$$-\frac{1}{2\pi i} \oint_{|z-1|=\epsilon<1} \frac{z^{x_i - x_j - 1}}{(1-z)^{n_j - n_i}} dz.$$

If $n_i \geq n_j$, then these residues are zero. If $n_i < n_j$, then $t_i < t_j$, which implies $x_i > x_j$, so the integral in z from expression (4) is zero. So when $n_i < n_j$, the extra term can be written as

$$(-1)^{n_j - n_i - 1} \binom{x_i - x_j - 1}{n_j - n_i - 1} = (-1)^{n_j - n_i - 1} \binom{x_i - x_j}{n_j - n_i} \frac{n_j - n_i}{x_i - x_j}.$$

Using Laplace-Demoivre, this binomial converges to 16. So expression (17) holds.

Case 3: $-1 < c_1 < 0$. If a and b are small enough, then $Q_{a,b}$ has two roots between -1 and 0. The second row in Figure 15 corresponds to the smaller root, while the third row corresponds to the larger root. In the second row p_3 is positive, while in the third row p_3 is negative. In both rows $z_1 < 0$.

Making the deformations gives residues at $u = w$, which can be written as

$$-\frac{1}{2\pi i}\oint_{|z|=r<1} \frac{z^{x_i-x_j-1}}{(1-z)^{n_j-n_i}}dz.$$

If $n_i \leq n_j$, then this expression cancels with the z-integral in expression (5). If $n_i > n_j$, then the extra term can be written as

$$-(-1)^{x_j-x_i}\binom{n_i-n_j}{x_j-x_i}.$$

Once again, this converges to expression (16). So expression (17) holds. □

References

[1] A. Aptekarev, P. Bleher, and A. Kuijlaars, *Large n limit of Gaussian random matrices with external source, part II*, Comm. Math. Phys. **259** (2005), no. 2, 367-389. arXiv:math-ph/0408041v1

[2] J. Baik, P. Deift, and K. Johansson, *On the distribution of the length of the longest increasing subsequence of random permutations*, J. Amer. Math. Soc. **12** (1999), no. 4, 1119-1178. arXiv:math/9810105v2.

[3] J. Baik, P. Deift, and K. Johansson, *On the distribution of the length of the second row of a Young diagram under Plancherel measure*, Geom. Funct. Anal. **10** (2000), no. 4, 702-731. arXiv:math/9901118v1

[4] P. Biane, *Approximate factorization and concentration for characters of symmetric groups*, Inter. Math. Res. Notices **2001** (2001), no. 4, 179-192.

[5] A. Borodin. *Periodic Schur Process and Cylindric Partitions*, Duke Math. J. Volume 140, Number 3 (2007), 391-468. arXiv:math/0601019v1

[6] A. Borodin and P. Ferrari, *Large time asymptotics of growth models on space-like paths I: PushASEP*. arXiv:0707.2813v2

[7] A. Borodin, P. Ferrari, M. Prähofer, T. Sasamoto. *Fluctuation properties of the TASEP with periodic initial configuration*, to appear in Jour. Stat. Phys. arXiv:math-ph/0608056v3

[8] A. Borodin, A. Okounkov and G. Olshanski, *Asymptotics of Plancherel measures for symmetric groups*, J. Amer. Math. Soc. **13** (2000), no. 3, 481-515. arXiv:math/9905032v2

[9] A. Borodin and G. Olshanski, *Harmonic analysis on the infinite-dimensional unitary group and determinantal point processes*, Ann. of Math. (2) **161** (2005), no. 3, 1319-1422. arXiv:math/0109194v2

[10] A. Borodin and G. Olshanski, *Representation theory and random point processes*, European Congress of Mathematics, 73-94, Eur. Math. Soc., Zrich, 2005. arXiv:math/0409333v1

[11] A. Borodin and G. Olshanski. *Stochastic dynamics related to Plancherel measure on partitions*, Amer. Math. Soc., Translations – Series 2, vol. 217, 2006, 9-22. arXiv:math-ph/0402064v2

[12] A. Borodin and G. Olshanski, *Asymptotics of Plancherel-type random partitions*, J. Algebra **313** (2007), no. 1, 40-60. arXiv:math/0610240v2

[13] E. Brezin and S. Hikami, *Level Spacing of Random Matrices in an External Source*, Phys. Rev. E (3) **58** (1998), no. 6, part A, 7176-7185. arXiv:cond-mat/9804024v1

[14] E. Brezin and S. Hikami, *Universal singularity at the closure of a gap in a random matrix theory*, Phys. Rev. E (3) **57** (1998), no. 4, 4140-4149. arXiv:cond-mat/9804023v1

[15] K. Johansson, *Discrete Polynuclear Growth and Determinantal Processes*, Comm. Math. Phys., **242** (2003), 277-329. arXiv:math/0206208v2

[16] K. Johansson, *Discrete orthogonal polynomial ensembles and the Plancherel measure*, Ann. of Math. (2) **153** (2001), no. 1, 259-296. arXiv:math/9906120v3

[17] S. V. Kerov, *Asymptotic Representation Theory of the Symmetric Group and Its Applications in Analysis*, volume 219 of Translations of Mathematical Monographs. Amer. Math. Soc., 2003.

[18] S. V. Kerov, *Distribution of symmetry types of high rank tensors*, Zapiski Nauchnyh Seminarov LOMI **155** (1986), 181-186(Russian); English translation in J. Soviet Math. (New York) **41** (1988), no. 2, 995-999.

[19] B. F. Logan and L. A. Shepp, *A variational problem for random Young tableaux*, Adv. Math., **26**, 1977, 206-222.

[20] A. Okounkov, *Symmetric functions and random partitions*, Symmetric functions 2001: surveys of developments and perspectives, 223-252, NATO Sci. Ser. II Math. Phys. Chem., 74, Kluwer Acad. Publ., Dordrecht, 2002. arXiv:math/0309074v1

[21] A. Okounkov, *Random Matrices and Random Permutations*, Internat. Math. Res. Notices 2000, no. 20, 1043-1095. arXiv:math/9903176v3

[22] A. Okounkov and G. Olshanski, *Asymptotics of Jack polynomials as the number of variables goes to infinity,* Intern. Math. Res. Notices (1998), no. 13, 641-682.

[23] A. Okounkov and N. Reshetikhin, *Correlation function of Schur process with application to local geometry of a random 3-dimensional Young diagram*, J. Amer. Math. Soc. **16** (2003), no. 3, 581-603. arXiv:math/0107056v3

[24] A. Okounkov and N. Reshetikhin, *Random skew plane partitions and the Pearcey process*, Comm. Math. Phys. **269** (2007), no. 3, 571-609. arXiv:math/0503508v2

[25] G. Olshanski, *The problem of harmonic analysis on the infinite dimensional unitary group,* J. Funct. Anal. **205** (2003), no. 2, 464-524. arXiv:math/0109193v1

[26] M. Prähofer and H. Spohn, *Scale Invariance of the PNG Droplet and the Airy Process*, J. Stat. Phys. 108 (5-6): 1071-1106 (2002). arXiv:math/0105240v3

[27] C. Tracy and H. Widom, *The Pearcey Process*, Commun. Math. Phys. 263, 381-400 (2006). arXiv:math/0412005v3.

[28] A. Vershik and S. Kerov, *Asymptotics of the Plancherel measure of the symmetric group and the limit form of Young tableaux*, Soviet Math. Dokl., **18**, 1977, 527-531.

[29] A. Vershik and S. Kerov, *Characters and factor representations of the infinite unitary group,* Soviet Math. Doklady **26** (1982), 570-574.

[30] A. Vershik and S. Kerov, *Asymptotics of the maximal and typical dimension of irreducible representations of symmetric group*, Func. Anal. Appl., **19**, 1985, no.1, 25-36.

[31] D. Voiculescu, *Représentations factorielles de type II_1 de $U(\infty)$*, J. Math Pures et Appl. **55** (1976), 1-20.

[32] D. P. Zhelobenko, *Compact Lie groups and their representations*, Nauka, Moscow, 1970 (Russian); English translation: Transl. Math. Monographs **40**, Amer. Math. Soc., Providence, R.I., 1973.